View metadata, citation and similar papers at core.ac.uk

brought to you by CORE

provided by Brunel University Research Archive

CERN-PH-EP/2013-195
2014/01/22

CMS-FSQ-12-022

arXiv:1310.4554v2 [hep-ex] 13 Dec 2013

Jet and underlying event properties as a function of charged-particle multiplicity in proton-proton collisions at $\sqrt{s} = 7\,\text{TeV}$

The CMS Collaboration*

Abstract

Characteristics of multi-particle production in proton-proton collisions at $\sqrt{s} = 7\,\text{TeV}$ are studied as a function of the charged-particle multiplicity, N_{ch}. The produced particles are separated into two classes: those belonging to jets and those belonging to the underlying event. Charged particles are measured with pseudorapidity $|\eta| < 2.4$ and transverse momentum $p_{\text{T}} > 0.25\,\text{GeV}/c$. Jets are reconstructed from charged-particles only and required to have $p_{\text{T}} > 5\,\text{GeV}/c$. The distributions of jet p_{T}, average p_{T} of charged particles belonging to the underlying event or to jets, jet rates, and jet shapes are presented as functions of N_{ch} and compared to the predictions of the PYTHIA and HERWIG event generators. Predictions without multi-parton interactions fail completely to describe the N_{ch}-dependence observed in the data. For increasing N_{ch}, PYTHIA systematically predicts higher jet rates and harder p_{T} spectra than seen in the data, whereas HERWIG shows the opposite trends. At the highest multiplicity, the data–model agreement is worse for most observables, indicating the need for further tuning and/or new model ingredients.

Published in the European Physical Journal C as doi:10.1140/epjc/s10052-013-2674-5.

© 2014 CERN for the benefit of the CMS Collaboration. CC-BY-3.0 license

*See Appendix A for the list of collaboration members

1 Introduction

Achieving a complete understanding of the details of multi-particle production in hadronic collisions remains an open problem in high-energy particle physics. In proton-proton (pp) collisions at the energies of the Large Hadron Collider (LHC), most of the inelastic particle production is described in a picture in which an event is a combination of hadronic jets, originating from hard parton-parton interactions with exchanged momenta above several GeV/c, and of an underlying event consisting of softer parton-parton interactions, and of proton remnants.

The production of high-transverse-momentum jets, defined as collimated bunches of hadrons, results from parton cascades generated by the scattered quarks and gluons, described by perturbative quantum chromodynamics (QCD), followed by non-perturbative hadronization described either via color fields ("strings") stretching between final partons, or by the formation of colorless clusters of hadrons [1]. The underlying event (UE) is commonly defined as the set of all final-state particles that are not associated with the initial hard-parton scattering. This component is presumably dominated by perturbative (mini)jets with relatively small transverse momenta of a few GeV/c, produced in softer multi-parton interactions (MPI) [2–8], as well as by soft hadronic strings from the high-rapidity remnants. The description of the UE is more phenomenological than that of the jets arising from the primary hard-parton scatter, whose final hadron multiplicity can be in principle computed in QCD [1]. In this two-component approach, rare high-multiplicity events can be explained as due to a large number of MPI taking place in the pp collisions at small impact parameters. Different variants of such a physical picture are realized in state-of-the-art Monte Carlo (MC) event generators such as PYTHIA [9, 10] and HERWIG [11, 12]. The properties of multi-particle production are very sensitive to the assumptions made about the combination of MPI and hard scatterings, the modeling of the multi-parton interactions (in particular the transverse structure of the proton) [3], and non-perturbative final-state effects such as color reconnections, hadronization mechanisms, and possible collective-flow phenomena, among others.

Experimental data on multi-particle production in pp collisions at LHC energies provide a clear indication that our understanding of the different components contributing to the total inelastic cross section is incomplete. This arises from difficulties in describing multiplicity distributions, and especially the high-multiplicity tails [13], or in reproducing a new structure of the azimuthal angular correlations at 7 TeV for high-multiplicity events, the so-called "ridge" [14]. Interesting disagreements between data and MC simulation were also recently reported in transverse sphericity analyses and for global event shapes [15–17]. Together with similar findings in nucleus-nucleus collisions, these disagreements point to the intriguing possibility of some mechanisms at high multiplicities which are not properly accounted for in event generator models. Therefore, although the standard mixture of (semi)hard and non-perturbative physics considered by PYTHIA and HERWIG is often sufficient for reproducing the bulk properties of inelastic events, it fails to provide a more detailed description of the data and in particular of the properties of events binned in particle multiplicity.

The average transverse momentum of the charged particles produced in pp and $\mathrm{p\bar{p}}$ collisions has been measured as a function of the event multiplicity at various center-of-mass energies [13, 18–22]. The work presented here is the first one that carries out the study also for the UE and jets separately and includes other observables (jet p_{T} spectra, rates and shapes) not analyzed before as a function of particle multiplicity with such a level of detail.

The paper is organized as follows. The general procedure of the analysis is described in Section 2, a short description of the Compact Muon Solenoid (CMS) detector is given in Section 3, and the event generator models used are presented in Section 4. Sections 5 to 7 describe trigger

and event selection, track and jet reconstruction, the data correction procedure, and the systematic uncertainties. Results and discussions are presented in Section 8, and summarized in Section 9.

2 Analysis strategy

The main goal of this analysis is to study the characteristic features and relative importance of different mechanisms of multi-particle production in pp collisions at a center-of-mass energy of $\sqrt{s} = 7\,\text{TeV}$ in different charged-particle multiplicity bins, corresponding to different levels of hadronic activity resulting from larger or smaller transverse overlap of the colliding protons. Guided by the two-component physical picture described in the introduction, we separate the particle content of each inelastic event into two subsets. We identify the jet-induced contribution and treat the rest as the underlying event originating from unresolved perturbative sources such as semihard MPI and other softer mechanisms. Our approach to this problem uses the following procedure, applied at the stable (lifetime $c\tau > 10\,\text{mm}$) particle-level:

- Similarly to the centrality classification of events in high-energy nuclear collisions [23], events are sorted according to their charged-particle multiplicity (Table 1). Hereafter, for simplicity, multiplicity should always be understood as charged-particle multiplicity.
- For each event, jets are built with charged particles only using the anti-k_T algorithm [24, 25] with a distance parameter 0.5, optimized as described below, and are required to have a $p_\text{T} > 5\,\text{GeV}/c$. Charged particles falling within a jet cone are labeled as "intrajet particles".
- After removing all intrajet particles from the event, the remaining charged particles are defined as belonging to the underlying event. Events without jets above $p_\text{T} = 5\,\text{GeV}/c$ are considered to consist of particles from the UE only.

In order to achieve a better separation of the contributions due to jets and underlying event, the resolution parameter of the anti-k_T algorithm is increased until the UE charged-particle p_T-spectrum starts to saturate, indicating that the jet component has been effectively removed. This way of fixing the jet cone radius minimizes contamination of the underlying event by jet contributions or vice versa. A resolution parameter of value 0.5 is found to be optimal. Of course, it is not possible to completely avoid mixing between jets and underlying event. To clarify the picture and minimize the mixing of the two components, we measure not only the p_T spectrum of the charged particles inside jet cones, but also the spectrum of the leading (the highest-p_T) charged particle in each cone.

3 The CMS detector

A detailed description of the CMS detector can be found in Ref. [26]. A right-handed coordinate system with the origin at the nominal interaction point (IP) is used, with the x axis pointing to the center of the LHC ring, the y axis pointing up, and the z axis oriented along the anticlockwise-beam direction. The central feature of the CMS detector is a superconducting solenoid of 6 m internal diameter providing an axial magnetic field with a nominal strength of 3.8 T. Immersed in the magnetic field are the pixel tracker, the silicon-strip tracker, the lead tungstate electromagnetic calorimeter, the brass/scintillator hadron calorimeter, and the muon detection system. In addition to the barrel and endcap calorimeters, the steel/quartz-fibre forward calorimeter covers the pseudorapidity region $2.9 < |\eta| < 5.2$, where $\eta = -\log[\tan(\theta/2)]$,

and θ is the polar angle measured at the center of the CMS detector with respect to the z axis. The tracking detector consists of 1440 silicon-pixel and 15 148 silicon-strip detector modules. The barrel part consists of 3 (10) layers of pixel (strip) modules around the IP at distances ranging from 4.4 cm to 1.1 m. Five out of the ten strip layers are double-sided and provide additional z coordinate measurements. The two endcaps consist of 2 (12) disks of pixel (strip) modules that extend the pseudorapidity acceptance to $|\eta| = 2.5$. The tracker provides an impact parameter resolution of about 100 μm and a p_{T} resolution of about 0.7% for 1 GeV/c charged particles at normal incidence. Two of the CMS subdetectors acting as LHC beam monitors, the Beam Scintillation Counters (BSC) and the Beam Pick-up Timing for the eXperiments (BPTX) devices, are used to trigger the detector readout. The BSC are located along the beam line on each side of the IP at a distance of 10.86 m and cover the range $3.23 < |\eta| < 4.65$. The two BPTX devices, which are located inside the beam pipe and $\pm$175 m from the IP, are designed to provide precise information on the structure and timing of the LHC beams with a time resolution of 0.2 ns.

4 Event generator models

The best available general-purpose event generators and their tunes are used for comparison with the data. They are the PYTHIA 6 (version 6.424 [9], tune Z2*), PYTHIA 8 (version 8.145 [10], tune 4C [27]), and HERWIG++ 2.5 (tune UE-EE-3M) [12] event generators. These event generators and tunes differ in the treatment of initial and final state radiation, hadronization, and in the choice of underlying event parameters, color reconnections, and cutoff values for the MPI mechanism. Values of these parameters were chosen to provide a reasonable description of existing LHC pp differential data measured in minimum-bias and hard QCD processes. Initial and final state radiation is essential for the correct description of jet production and of the UE [28]. For the MPI modeling, PYTHIA incorporates interleaved evolution between the different scatterings [27, 29], whereas HERWIG concentrates more hard scatterings at the center of the pp collision while allowing for more (disconnected) soft-parton scatterings at the periphery. A detailed review of the implementation of all these mechanisms in modern MC event generators is given [30]. The most recent PYTHIA 6 Z2* tune is derived from the Z1 tune [31], which uses the CTEQ5L parton distribution set, whereas Z2* adopts CTEQ6L [32]. The Z2* tune is the result of retuning the PYTHIA parameters PARP(82) and PARP(90) by means of the automated PROFESSOR tool [33], yielding PARP(82)=1.921 and PARP(90)=0.227. The results of this study are also compared to predictions obtained with PYTHIA 8, tune 4C, with multi-parton interactions switched off. Hadronization in PYTHIA is based on the Lund string model [2] while that in HERWIG is based on the cluster fragmentation picture in which perturbative evolution forms preconfined clusters that subsequently decay into final hadrons. The version of HERWIG++ 2.5 UE-EE-3M used in this paper includes important final-state effects due to color reconnections and is based on the MRST2008 parton distribution set [34].

5 Event selection and reconstruction

The present analysis uses the low-pileup data recorded during the first period of 2010 data taking, corresponding to an integrated luminosity of $(3.18 \pm 0.14)\,\mathrm{pb}^{-1}$. The data are collected using a minimum-bias trigger requiring a signal from both BPTX detectors coincident with a signal from both BSC detectors.

For this analysis, the position of the reconstructed primary vertex is constrained to be within $\pm$10 cm with respect to the nominal IP along the beam direction and within $\pm$2 cm in the transverse direction, thereby substantially rejecting non-collision events [35]. The fraction of back-

ground events after these selections is found to be negligible (<0.1%).

The fraction of events in the data sample with pileup (two or more pp collisions per bunch crossing) varies in the range (0.4–7.8)% depending on the instantaneous luminosity per bunch. This small fraction of pileup events is kept, but the analysis is only carried out for the tracks connected with the primary (highest multiplicity) vertex. The fraction of events where two event vertices are reconstructed as one, or where two event vertices share associated tracks, ranges between (0.04–0.2)%.

5.1 Track reconstruction and selection

The track reconstruction procedure uses information from both pixel and strip detectors and is based on an iterative combinatorial track finder [36]. Tracks are selected for analysis if they have transverse momenta $p_{\mathrm{T}} > 0.25\,\mathrm{GeV}/c$ and pseudorapidities lying within the tracker acceptance $|\eta| < 2.4$. Such p_{T} cut provides robust measurements, keeping the event selection minimally biased by hard processes. In addition, tracks must be associated with the event vertex with the highest multiplicity in the bunch crossing. The requirement removes tracks coming from secondary interactions with detector materials, decays of long-lived neutral hadrons, and pileup. Residual contamination from such tracks is at the level of 0.2%.

5.2 Charged-particle jet reconstruction

This analysis is based on jets that are reconstructed using tracks only, in order to avoid the reconstructed jet energy uncertainty due to mismeasurements of low-p_{T} neutral particles. Jets are reconstructed by clustering the tracks with the collinear- and infrared-safe anti-k_{T} algorithm with a distance parameter of 0.5, that results in cone-shaped jets. Jets are retained if their axes lie within the fiducial region $|\eta^{\text{jet axis}}| < 1.9$, so that for a jet with an effective radius of 0.5 all jet constituent tracks fall within the tracker acceptance ($|\eta| < 2.4$).

6 Data correction

6.1 Event selection efficiency

In the MC simulations, events are selected at the stable-particle level (lifetime $c\tau > 10\,\mathrm{mm}$) if at least one charged particle is produced on each side of the interaction point within $3.32 < |\eta| < 4.65$, mimicking the BSC trigger requirement, and, in addition, if at least five charged particles with $p_{\mathrm{T}} > 0.25\,\mathrm{GeV}/c$ and $|\eta| < 2.4$ are present, which ensures a high vertex finding efficiency in the offline selection of data.

The trigger efficiency is measured using data collected with a zero-bias trigger, constructed from a coincidence of the BPTX counters, which effectively requires only the presence of colliding beams at the interaction point. The offline selection efficiency is determined from MC simulations. The combined trigger and offline selection efficiency is obtained as a function of the number of reconstructed tracks and is very high: above 87% for events with more than 10 reconstructed tracks and close to 100% for events with more than 30 reconstructed tracks. Results are corrected by applying a weight inversely proportional to the efficiency to each observed event.

6.2 Corrections related to the track reconstruction

The track-based quantities (N_{ch}, average p_{T} of tracks, jet p_{T} density in ring zones) are corrected in a two-stage correction procedure. First, each observed track is given a weight to account for

Table 1: Charged-particle multiplicity bins, mean charged-particle multiplicity in bins, and corresponding number of events. The multiplicity N_{ch} is defined as the total number of stable charged-particles in the events, corrected for inefficiencies, with transverse momentum $p_{\mathrm{T}} > 0.25\,\mathrm{GeV}/c$ and pseudorapidity $|\eta| < 2.4$.

Multiplicity range	Mean multiplicity $\langle N_{\mathrm{ch}} \rangle$	Number of events
$10 < N_{\mathrm{ch}} \leq 30$	18.9	2 795 688
$30 < N_{\mathrm{ch}} \leq 50$	38.8	1 271 987
$50 < N_{\mathrm{ch}} \leq 80$	61.4	627 731
$80 < N_{\mathrm{ch}} \leq 110$	90.6	105 660
$110 < N_{\mathrm{ch}} \leq 140$	120	11 599

track reconstruction inefficiencies and misreconstructed (fake) track rates, as obtained from the detector simulation. The weights are based on two-dimensional matrices $\epsilon(\eta, p_{\mathrm{T}})$ and $f(\eta, p_{\mathrm{T}})$, for reconstruction efficiency and fake track rates, respectively, computed in bins in η, p_{T}, and is given by

$$N_{\mathrm{ch}}^{\mathrm{true}}(\eta, p_{\mathrm{T}}) = N_{\mathrm{ch}}^{\mathrm{reco}}(\eta, p_{\mathrm{T}}) \frac{1 - f(\eta, p_{\mathrm{T}})}{\epsilon(\eta, p_{\mathrm{T}})}. \tag{1}$$

The corrections for reconstruction efficiencies and fake rates depend on track multiplicity. Therefore, four different sets of matrices $\epsilon(\eta, p_{\mathrm{T}})$ and $f(\eta, p_{\mathrm{T}})$ for different track multiplicity classes are used, the first three track multiplicity classes corresponding to the first three charged-particle multiplicity bins of Table 1 and the fourth one corresponding to the fourth and fifth charged-particle multiplicity bins. The average track reconstruction efficiency and fake rate vary between 79–80% and 3–4%, respectively, depending on the multiplicity bin considered.

Table 1 shows the corrected charged-particle multiplicity classes used in this analysis and the number of events and mean multiplicities in each multiplicity bin after applying all event selection criteria.

Figure 1 shows multiplicity distributions that have been corrected for tracking efficiency and fake rate. The simulations fail to describe all the measured N_{ch} distributions, as discussed in Ref. [13]. As we are considering event properties as a function of multiplicity, such a data–MC disagreement might introduce a bias due to the different N_{ch} distribution within the wide multiplicity intervals. Reweighting the multiplicity distributions in MC simulations to bring them in agreement with the ones observed in data results in less than 1–2% corrections for all results. In the following, corrected results are compared to the predictions obtained from the unweighted MC models.

All the measured quantities hereafter are further corrected to stable-particle level using a bin-by-bin factor obtained from Monte Carlo simulations. This correction factor accounts for event migration between adjacent multiplicity bins, for differences in the tracking performance in the dense environment inside jets, and for mixing between charged particles belonging to charged-particle jets and the UE due to jets that are misidentified at the detector level. The magnitude of this correction factor is typically less than 1%, except for the jet p_{T} density in the core of the jet where it reaches up to 8%.

6.3 Correction of the track-jet p_{T} distributions

Track-jet distributions have to be corrected for inefficiencies in reconstruction, for misidentified jets, and for bin migrations due to the finite energy resolution. On average, a reconstructed

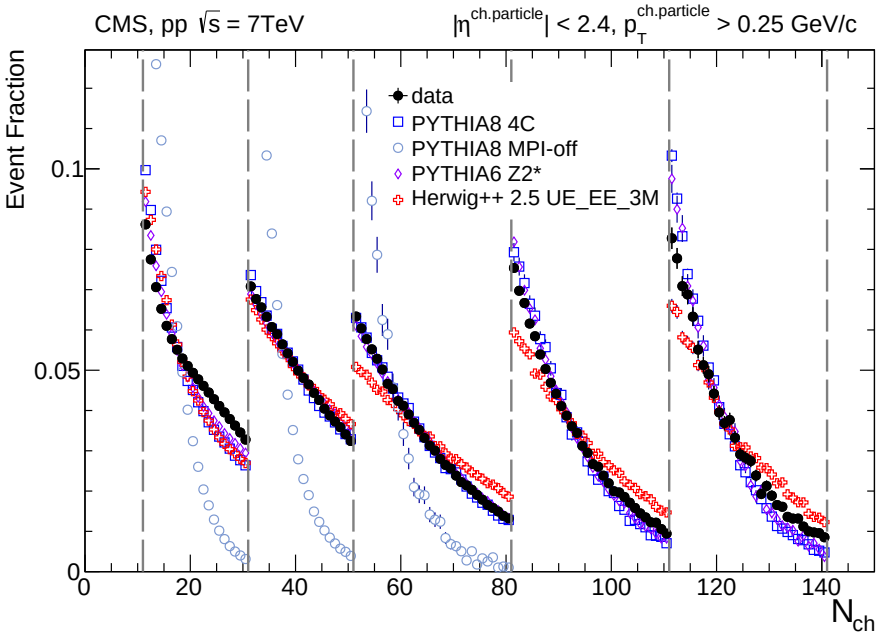

Figure 1: Charged-particle multiplicity distributions, corrected for tracking efficiency and fake rate, for the five multiplicity bins defined in this analysis compared to four different MC predictions. The normalization is done for each multiplicity bin separately. PYTHIA 8 with MPI switched off completely fails to produce events at large multiplicity and therefore no points are shown in the two highest multiplicity domains.

track-jet has 95% of the energy of the original charged-particle jet. The energy resolution of such jets is about 13%. The reconstructed jet spectrum is related to the "true" jet spectrum as follows:

$$M(p_{\mathrm{T}}^{\mathrm{measured}}) = \int C(p_{\mathrm{T}}^{\mathrm{measured}}, p_{\mathrm{T}}^{\mathrm{true}}) T(p_{\mathrm{T}}^{\mathrm{true}}) \mathrm{d}p_{\mathrm{T}}^{\mathrm{true}}, \tag{2}$$

where $M(p_{\mathrm{T}}^{\mathrm{measured}})$ and $T(p_{\mathrm{T}}^{\mathrm{true}})$ are the measured and the true p_{T} spectra, respectively, and $C(p_{\mathrm{T}}^{\mathrm{measured}}, p_{\mathrm{T}}^{\mathrm{true}})$ is a response function obtained from the MC simulation. The problem of inverting the response relation of Eq. (2) is well known and has been extensively studied in literature. In our analysis, an iterative unfolding technique [37] is applied. Since the detector response changes with multiplicity, individual response matrices are used for each multiplicity bin.

7 Systematic uncertainties

The following sources of systematic uncertainties are considered:

Association of tracks with the primary vertex (track selection): Tracks that are coming from a non-primary interaction result in an incorrect multiplicity classification of the event and bias the event properties at a given multiplicity. These tracks originate from secondary interactions with detector material, decays of long-lived neutral hadrons, and pileup. Moreover, these tracks can bias the p_{T} spectrum of primary tracks. As it is not possible to completely avoid contamination by such tracks, the stability of the results has been estimated by tightening and loosening the association criteria. Removing contamination inevitably leads to rejection of some valid primary tracks, so for each set of the association criteria a special efficiency and fake-rate correction must be used.

Table 2: Summary of systematic and statistical uncertainties for various averaged inclusive and UE-related quantities. The variables $\langle p_{\mathrm{T}}^{\text{ch. particle}} \rangle$, $\langle p_{\mathrm{T}}^{\mathrm{UE}} \rangle$, $\langle PT^{\mathrm{ij}} \rangle$, $\langle p_{\mathrm{T}}^{\mathrm{ijl}} \rangle$ are defined in Section 8.1, $\rho(R)$ is defined in Section 8.2.3.

	$\langle p_{\mathrm{T}}^{\text{ch. particle}} \rangle$	$\langle p_{\mathrm{T}}^{\mathrm{UE}} \rangle$	$\langle p_{\mathrm{T}}^{\mathrm{ij}} \rangle$	$\langle p_{\mathrm{T}}^{\mathrm{ijl}} \rangle$	$\rho(R)$
Track selection	<0.2%	<0.2%	<0.2%	<0.4%	<1%
Tracking performance	<0.3%	<0.3%	<0.4%	<0.4%	<4%
Model dependence	<0.5%	<0.4%	<0.5%	<0.5%	<5%
Statistical	<0.1%	<0.1%	<0.2%	<0.4%	2–8%
Total	0.5–0.7%	0.5–0.6%	0.5–0.7%	<0.9%	4–9%

Tracking performance: A correct description of the tracking performance in the MC simulation of the detector is essential. A conservative estimate of the uncertainty of this efficiency of 2.3% is taken from Ref. [38].

Model dependence of the correction procedures: Different MC models can give slightly different detector and reconstruction responses. Two models, PYTHIA 6 tune Z2* and PYTHIA 8 tune 4C, are used to compute tracking and jet performance and correction factors. HERWIG++ 2.5 was found to deviate too much from the data and was not used for the estimate of the systematic uncertainty. Corrections based on the PYTHIA 6 tune Z2* model, which provides better agreement with data, are used to get the central values of different physics quantities. The differences between these two methods are assigned as a systematic uncertainty.

Unfolding the jet p_{T} spectrum: The unfolding procedure used to correct for bin migrations in the jet p_{T} spectra is based on an iterative unfolding technique [37] for which we find that 4–5 iterations are optimal. By varying the number of iterations (± 1 with respect to the optimal value) and the reconstructed-to-generated jet matching parameter ($0.15 < \Delta R < 0.25$) we obtain a systematic uncertainty of $(0.5 - 2.0)\%$. This leads to a systematic uncertainty <0.2% in the average p_{T} of the jet spectrum, and <2% for charged-particle jet rates.

Although this analysis uses a low-pileup data sample, rare high-multiplicity events might occur due to overlapping pp collisions in the same bunch crossing. The effect of pileup is estimated by comparing results at different instantaneous luminosities. The dataset is divided into subsets according to the instantaneous luminosity and the differences found between these subsets are of the order of the statistical uncertainties of the sample. In addition, it was checked that the instantaneous luminosity for events with small and large N_{ch} does not differ, confirming that the large-multiplicity bins are not biased by a possibly increased contribution from pileup events. Therefore, we conclude that high-multiplicity events are not affected by pileup.

Tables 2 and 3 summarize the systematic and statistical uncertainties of the measured quantities. The total uncertainties are the sum in quadrature of the individual systematic and statistical uncertainties. The total error of jet p_{T} density as a function of jet radius rises with R and N_{ch}. The total uncertainties in the jet p_{T} spectra are of the order of 4–8% for jet p_{T} up to about 25 GeV/c. For jets with $p_{\mathrm{T}} > 25$ GeV/c the statistical uncertainties dominate.

8 Results

8.1 General properties of charged particles from jets and from the UE

We start with discussing the general jet and UE properties in the five N_{ch} bins defined. Tables 4, 5 list the average transverse momentum for the various types of charged particles measured, as well as the predictions from PYTHIA 8 tune 4C, PYTHIA 8 MPI-off, PYTHIA 6 tune Z2*,

Table 3: Summary of systematic and statistical uncertainties for various charged-jet related quantities.

	ch. jet p_{T} spectrum	ch. jet rate ($p_{\mathrm{T}} > 5\,\mathrm{GeV}/c$)	ch. jet rate ($p_{\mathrm{T}} > 30\,\mathrm{GeV}/c$)	$\langle p_{\mathrm{T}}^{\text{ch. jet}} \rangle$
Track selection	<1%	<2%	<4%	<0.1%
Tracking performance	<3%	2%	<5%	<0.5%
Model dependence	<3%	2%	<6%	<0.4%
Unfolding	3%	<2%	<3%	<0.2%
Statistical	1–8% ($p_{\mathrm{T}}^{\text{ch. jet}} < 25\,\mathrm{GeV}/c$) 10–40% ($p_{\mathrm{T}}^{\text{ch. jet}} > 25\,\mathrm{GeV}/c$)	<1%	<9%	<0.4%
Total	4–10% ($p_{\mathrm{T}}^{\text{ch. jet}} < 25\,\mathrm{GeV}/c$) 10–40% ($p_{\mathrm{T}}^{\text{ch. jet}} > 25\ \mathrm{GeV}/c$)	<5%	<12%	0.8%

and HERWIG++ 2.5. For each multiplicity bin, we show the fully corrected results for the mean transverse momenta of all charged particles $\langle p_{\mathrm{T}}^{\text{ch. particle}} \rangle$, UE charged particles $\langle p_{\mathrm{T}}^{\mathrm{UE}} \rangle$, intrajet charged particles $\langle p_{\mathrm{T}}^{\mathrm{ij}} \rangle$, intrajet leading charged particles $\langle p_{\mathrm{T}}^{\mathrm{ijl}} \rangle$, the mean transverse momentum of charged-particle jets $\langle p_{\mathrm{T}}^{\text{ch. jet}} \rangle$, and the average number of jets per event $\langle \frac{\#\text{jets}}{\text{event}} \rangle$.

The mean transverse momenta of all charged particles, UE charged-particles, and intrajet charged-particles, are plotted as a function of N_{ch} in Figs. 2–4. From Figs. 2 and 3, we see that mean transverse momentum of inclusive and UE charged-particles increases with N_{ch}. Such a behavior is expected as the higher multiplicity events have an increased fraction of (semi)hard scatterings contributing to final hadron production. The (logarithmic-like) N_{ch}-dependence of the average transverse momentum of inclusive and UE charged-particles is well described by both PYTHIA 6 tune Z2* and PYTHIA 8 tune 4C (especially by the former), and is less well described by HERWIG++ 2.5, which does not predict a monotonically rising dependence but a "turn down" beyond $N_{\mathrm{ch}} \approx 60$. On the other hand, PYTHIA 8 without MPI fails to describe the data altogether, predicting much harder charged-particle spectra for increasing final multiplicity. This follows from the fact that PYTHIA 8 without MPI can only produce high-multiplicity events through very hard jets with large intrajet multiplicity, instead of producing a larger number of semi-hard jets in the event.

From Figs. 4–5 it is clear that the N_{ch}-dependence of the average p_{T} of intrajet constituents and leading charged-particle of the jets shows the opposite behavior compared to that from the global and underlying events (Figs. 2–3) and decreases logarithmically with increasing multiplicities. Events with increasing multiplicities are naturally "biased" towards final-states resulting mostly from (mini)jets which fragment into a (increasingly) large number of hadrons. Since the produced hadrons share the energy of the parent parton, a larger amount of them results in overall softer intrajet- and leading-hadron p_{T} spectra. Part of the decrease of the intrajet mean p_{T} with multiplicity could be also due to extra soft UE contribution falling within the jet cones, which increases from about 5% for $N_{\mathrm{ch}} \approx 20$, to about 20% for $N_{\mathrm{ch}} \approx 120$, according to PYTHIA 6 tune Z2*. In terms of data-MC comparisons, we see that PYTHIA 6 tune Z2* and HERWIG++ 2.5 describe relatively well the N_{ch}-dependence of the intrajet and leading-particle average p_{T}, whereas PYTHIA 8 tune 4C produces harder mean charged-particle spectra at high multiplicities. The PYTHIA 8 predictions without MPI increase dramatically with N_{ch}, and fail

Table 4: Average transverse momenta for different types of charged particles (inclusive, underlying event, intrajet, leading intrajet). The quantities are compared with the MC predictions. Uncertainties smaller than the last significant digit are omitted.

	$\langle p_{\mathrm{T}}^{\text{ch. particle}} \rangle$, GeV/$c$	$\langle p_{\mathrm{T}}^{\mathrm{UE}} \rangle$, GeV/$c$	$\langle p_{\mathrm{T}}^{\mathrm{ij}} \rangle$, GeV/$c$	$\langle p_{\mathrm{T}}^{\mathrm{ijl}} \rangle$, GeV/$c$
$10 < N_{\mathrm{ch}} \leq 30$				
Data	0.68 ± 0.01	0.65 ± 0.01	1.90 ± 0.02	3.65 ± 0.05
PYTHIA 8 4C	0.67	0.64	1.83	3.48 ± 0.01
PYTHIA 8 MPI-off	0.72	0.66	1.93	3.73
PYTHIA 6 Z2*	0.67	0.65	1.86	3.59
HERWIG++ 2.5	0.68	0.65	1.81	3.41
$30 < N_{\mathrm{ch}} \leq 50$				
Data	0.75 ± 0.01	0.71 ± 0.01	1.64 ± 0.02	3.37 ± 0.04
PYTHIA 8 4C	0.77	0.72	1.62	3.25 ± 0.01
PYTHIA 8 MPI-off	1.06	0.75	1.99	4.28 ± 0.02
PYTHIA 6 Z2*	0.74	0.70	1.62	3.33
HERWIG++ 2.5	0.72	0.68	1.62	3.26
$50 < N_{\mathrm{ch}} \leq 80$				
Data	0.80 ± 0.01	0.74 ± 0.01	1.45 ± 0.01	3.15 ± 0.03
PYTHIA 8 4C	0.84	0.76	1.49	3.10
PYTHIA 8 MPI-off	1.47	0.80	2.22	5.17 ± 0.09
PYTHIA 6 Z2*	0.80	0.74	1.44	3.10
HERWIG++ 2.5	0.74	0.68	1.43	3.08
$80 < N_{\mathrm{ch}} \leq 110$				
Data	0.85 ± 0.01	0.76 ± 0.01	1.32 ± 0.01	2.96 ± 0.03
PYTHIA 8 4C	0.90	0.78	1.41	3.04 ± 0.01
PYTHIA 6 Z2*	0.85	0.76	1.33	2.97
HERWIG++ 2.5	0.74	0.66	1.28	2.94
$110 < N_{\mathrm{ch}} \leq 140$				
Data	0.88 ± 0.01	0.77 ± 0.01	1.24 ± 0.01	2.86 ± 0.03
PYTHIA 8 4C	0.95	0.79	1.36	3.05
PYTHIA 6 Z2*	0.90	0.77	1.29	3.05 ± 0.01
HERWIG++ 2.5	0.70	0.62	1.16	2.82 ± 0.01

Table 5: Average transverse momentum of charged-particle jets and charged-particle jet rates for two thresholds, $p_{\mathrm{T}} > 5\,\mathrm{GeV}/c$ and $p_{\mathrm{T}} > 30\,\mathrm{GeV}/c$. The quantities are compared with the MC predictions. Uncertainties smaller than the last significant digit are omitted.

	$\langle p_{\mathrm{T}}^{\text{ch. jet}} \rangle$, GeV/$c$	$\langle \frac{\#\text{ch. jets}}{\text{event}} \rangle$ ($p_{\mathrm{T}}^{\text{ch. jet}} > 5\,\mathrm{GeV}/c$)	$\langle \frac{\#\text{ch. jets}}{\text{event}} \rangle$ ($p_{\mathrm{T}}^{\text{ch. jet}} > 30\,\mathrm{GeV}/c$)
		$10 < N_{\mathrm{ch}} \leq 30$	
Data	6.85 ± 0.06	0.054 ± 0.004	$(3.2 \pm 0.5) 10^{-5}$
PYTHIA 8 4C	7.08 ± 0.01	0.075	$(3.9 \pm 0.6) 10^{-5}$
PYTHIA 8 MPI-off	7.96 ± 0.01	0.152	$(2.03 \pm 0.02) 10^{-4}$
PYTHIA 6 Z2*	7.01 ± 0.01	0.067	$(2.7 \pm 0.3) 10^{-5}$
HERWIG++ 2.5	6.92 ± 0.01	0.095	$(3.8 \pm 0.5) 10^{-5}$
		$30 < N_{\mathrm{ch}} \leq 50$	
Data	7.04 ± 0.09	0.287 ± 0.014	$(3.4 \pm 0.4) 10^{-4}$
PYTHIA 8 4C	7.26 ± 0.01	0.386	$(4.4 \pm 0.5) 10^{-4}$
PYTHIA 8 MPI-off	10.8	1.38 ± 0.02	$(2.9 \pm 0.1) 10^{-2}$
PYTHIA 6 Z2*	7.20 ± 0.01	0.304	$(3.5 \pm 0.2) 10^{-4}$
HERWIG++ 2.5	7.02 ± 0.01	0.375	$(3.1 \pm 0.3) 10^{-4}$
		$50 < N_{\mathrm{ch}} \leq 80$	
Data	7.18 ± 0.09	0.84 ± 0.03	$(1.5 \pm 0.1) 10^{-3}$
PYTHIA 8 4C	7.41 ± 0.01	1.09	$(1.8 \pm 0.1) 10^{-3}$
PYTHIA 8 MPI-off	16.3 ± 0.4	3.1 ± 0.3	$(3.7 \pm 0.1) 10^{-1}$
PYTHIA 6 Z2*	7.30 ± 0.01	0.87	$(1.4 \pm 0.1) 10^{-3}$
HERWIG++ 2.5	7.10 ± 0.01	0.88	$(5.9 \pm 0.5) 10^{-4}$
		$80 < N_{\mathrm{ch}} \leq 110$	
Data	7.46 ± 0.11	2.13 ± 0.09	$(4.3 \pm 0.4) 10^{-3}$
PYTHIA 8 4C	7.77 ± 0.02	2.54	$(7.1 \pm 0.6) 10^{-3}$
PYTHIA 6 Z2*	7.64 ± 0.01	2.12	$(5.7 \pm 0.2) 10^{-3}$
HERWIG++ 2.5	7.25 ± 0.01	1.66	$(1.2 \pm 0.1) 10^{-3}$
		$110 < N_{\mathrm{ch}} \leq 140$	
Data	7.81 ± 0.10	3.68 ± 0.15	$(1.0 \pm 0.1) 10^{-2}$
PYTHIA 8 4C	8.31 ± 0.03	4.46	$(2.5 \pm 0.1) 10^{-2}$
PYTHIA 6 Z2*	8.15 ± 0.02	3.95	$(2.1 \pm 0.1) 10^{-2}$
HERWIG++ 2.5	7.37 ± 0.01	2.41	$(1.9 \pm 0.2) 10^{-3}$

to describe the data. This can be explained by the fact that PYTHIA MPI-off enriches the increasing multiplicity range with events with hard partons only, whereas the other MC models include additional semi-hard parton interactions that soften the final hadron p_T spectra.

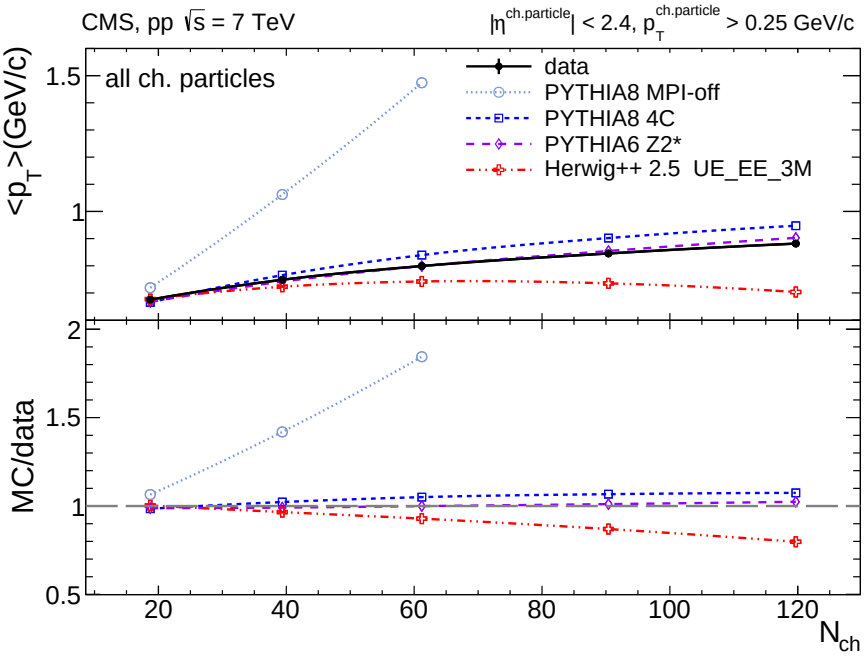

Figure 2: Mean transverse momentum of inclusive charged-particles with $p_T > 0.25\,\text{GeV}/c$ versus charged-particle multiplicity (N_{ch} within $|\eta| < 2.4$) measured in the data (solid line and marker) compared to various MC predictions (non-solid curves and markers). Systematic uncertainties are indicated by error bars which are, most of the time, smaller than the marker size.

8.2 Charged-particle jet properties

In the previous section, the jet substructure was investigated via the averaged properties of intrajet and leading particles. Now we turn to the description of the multiplicity-dependent properties of the jets themselves. In general, properties of inclusive jet production, when integrated over all multiplicities, are dominated by events with moderately low multiplicities, and are described quite well by QCD MC models [17, 39–41]. Here, we concentrate on the N_{ch}-dependence of a subset of jet properties, such as the number of jets per event, the mean transverse momenta of jets, differential jet p_T spectra, and jet widths.

Our study is complementary to others based on global event shapes, e.g. from the ALICE experiment [15], which observed an increasing event transverse sphericity as a function of multiplicity in contradiction with the MC predictions. However, the corresponding multiplicities are much lower in the ALICE study than in this analysis because of their smaller rapidity coverage ($|\eta| < 0.8$). Similar observations have been also recently seen by ATLAS [16], even though earlier CMS and ATLAS results show no serious disagreement with MC event generators [17, 40] as the events were not sorted according to their multiplicity. We show here that the higher sphericity of high-multiplicity events, relative to the PYTHIA predictions, is due to an apparent reduction and softening of the jet yields at high-N_{ch}.

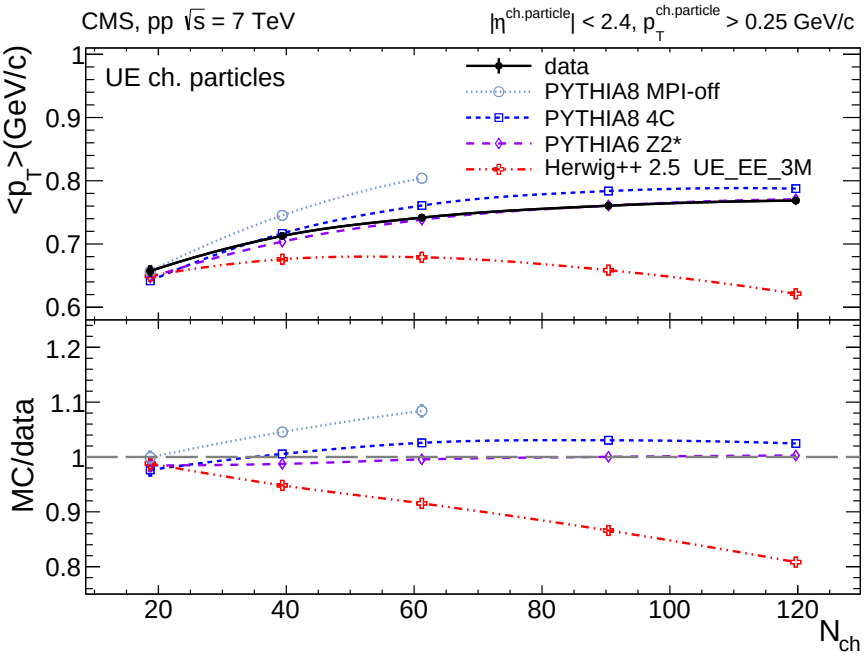

Figure 3: Mean transverse momentum of UE charged-particles with $p_{\mathrm{T}} > 0.25\,\mathrm{GeV}/c$ versus charged-particle multiplicity (N_{ch} within $|\eta| < 2.4$) measured in the data (solid line and marker) compared to various MC predictions (non-solid curves and markers). Systematic uncertainties are indicated by error bars which are, most of the time, smaller than the marker size.

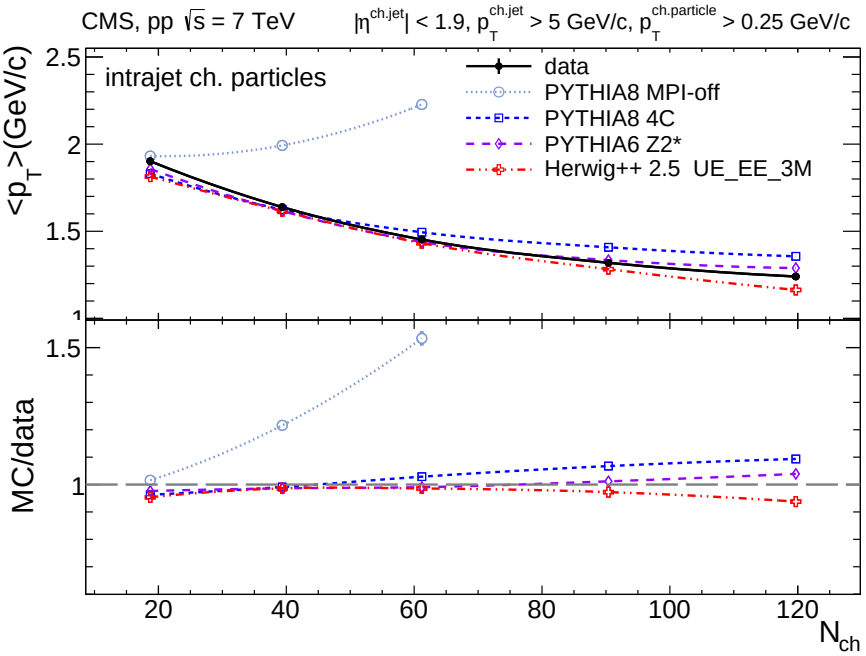

Figure 4: Mean transverse momentum of intrajet charged-particles with $p_{\mathrm{T}} > 0.25\,\mathrm{GeV}/c$ versus charged-particle multiplicity (N_{ch} within $|\eta| < 2.4$) measured in the data (solid line and marker) compared to various MC predictions (non-solid curves and markers). Systematic uncertainties are indicated by error bars which are, most of the time, smaller than the marker size.

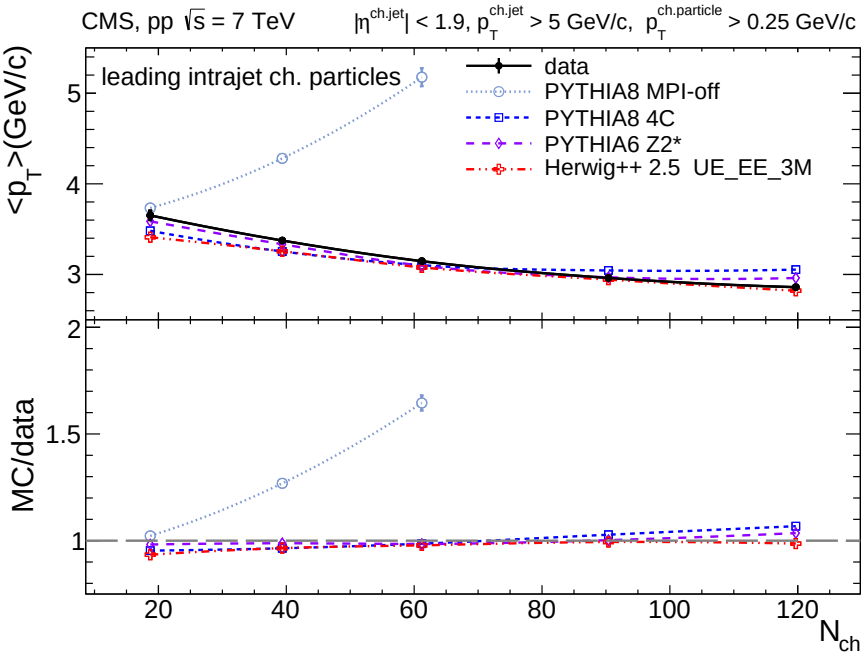

Figure 5: Mean transverse momentum of leading intrajet charged-particles with $p_{\mathrm{T}} > 0.25\,\mathrm{GeV}/c$ versus charged-particle multiplicity (N_{ch} within $|\eta| < 2.4$) measured in the data (solid line and marker) compared to various MC predictions (non-solid curves and markers). Systematic uncertainties are indicated by error bars which are, most of the time, smaller than the marker size.

8.2.1 Charged-particle jet production rates

The N_{ch}-dependence of the number of jets per event, with jet transverse momentum $p_{\mathrm{T}}^{\text{ch. jet}} > 5\,\mathrm{GeV}/c$ and $p_{\mathrm{T}}^{\text{ch. jet}} > 30\,\mathrm{GeV}/c$, is shown in Figs. 6 and 7, respectively.

For the small cutoff of $5\,\mathrm{GeV}/c$ the data show an increase from an average of 0.05 jets/event to about 4 jets/event going from the lowest to the highest charged-particle multiplicities. Such results, which confirm the importance of multiple (mini)jet production to explain the high-N_{ch} events, are very well described by PYTHIA 6 tune Z2*, while predictions of PYTHIA 8 tune 4C overestimate the rates at all N_{ch} and HERWIG ++ 2.5 underestimates them for increasing N_{ch}. For the higher $30\,\mathrm{GeV}/c$ cutoff, a large disagreement with the data is found in the higher-multiplicity bins (Fig. 7), where both versions of PYTHIA predict a factor of two more jets per event than seen in the data. On the contrary, HERWIG++ 2.5 predicts a factor of 5 fewer jets per event than experimentally measured. The prediction of PYTHIA 8 without MPI contributions is completely off-scale by factors of 3.5–6 above the data and is not shown in the plots.

The analysis of the N_{ch}-dependence of the mean transverse momentum of charged-particle jets $\langle p_{\mathrm{T}}^{\text{ch. jet}} \rangle$ is shown in Fig. 8. The average $\langle p_{\mathrm{T}}^{\text{ch. jet}} \rangle$ rises slowly with N_{ch} from about 7.0 to $7.7\,\mathrm{GeV}/c$, indicating a rising contribution from harder scatterings for increasingly "central" pp events. The predictions of PYTHIA 8 tune 4C, PYTHIA 6 tune Z2*, and HERWIG++ 2.5 are in good agreement with the data at low and intermediate multiplicities. However, the PYTHIA models display an increasingly higher value of $\langle p_{\mathrm{T}}^{\text{ch. jet}} \rangle$, i.e. a harder jet contribution, up to $8.4\,\mathrm{GeV}/c$ in the highest-multiplicity events.

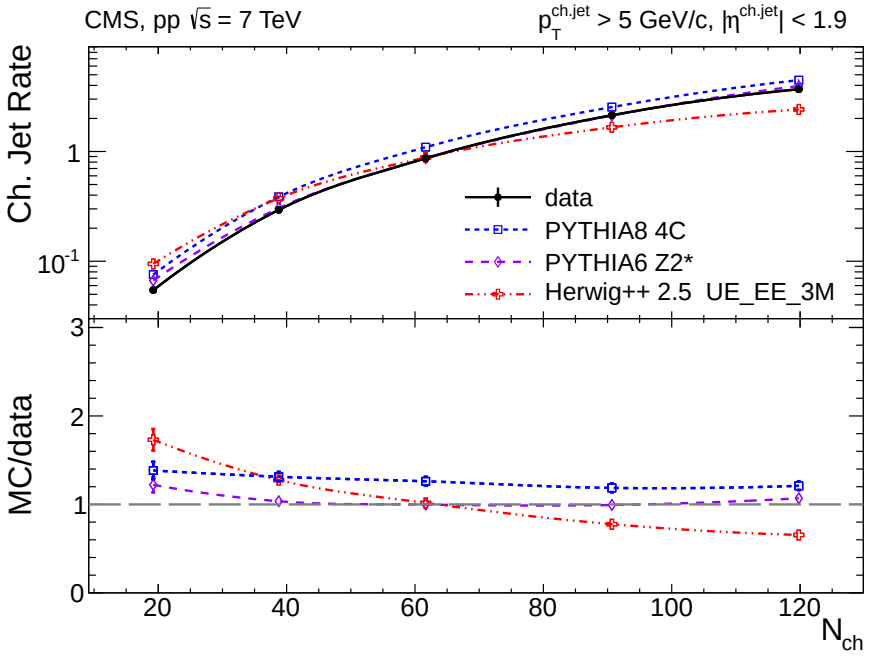

Figure 6: Number of charged-particle jets per event for $p_{\mathrm{T}}^{\text{ch. jet}} > 5\,\mathrm{GeV}/c$ and jet axes lying within $|\eta| < 1.9$ versus charged-particle multiplicity (N_{ch} within $|\eta| < 2.4$) measured in the data (solid line and marker) compared to various MC predictions (non-solid curves and markers). Systematic uncertainties are indicated by error bars which are, most of the time, smaller than the marker size.

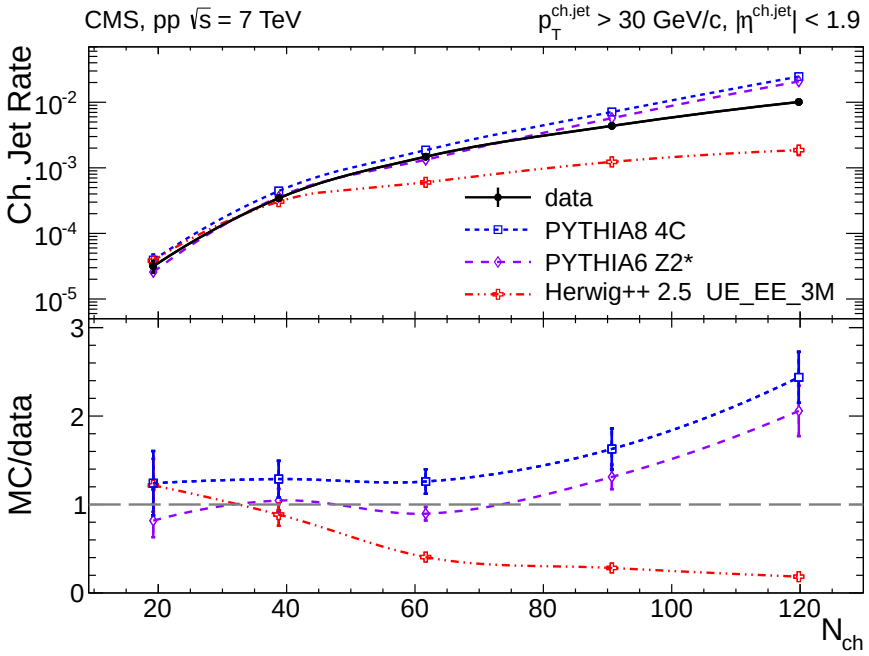

Figure 7: Number of charged-particle jets per event for $p_{\mathrm{T}}^{\text{ch. jet}} > 30\,\mathrm{GeV}/c$ and jet axes lying within $|\eta| < 1.9$ versus charged-particle multiplicity (N_{ch} within $|\eta| < 2.4$) measured in the data (solid line and marker) compared to various MC predictions (non-solid curves and markers). Error bars denote the total uncertainties.

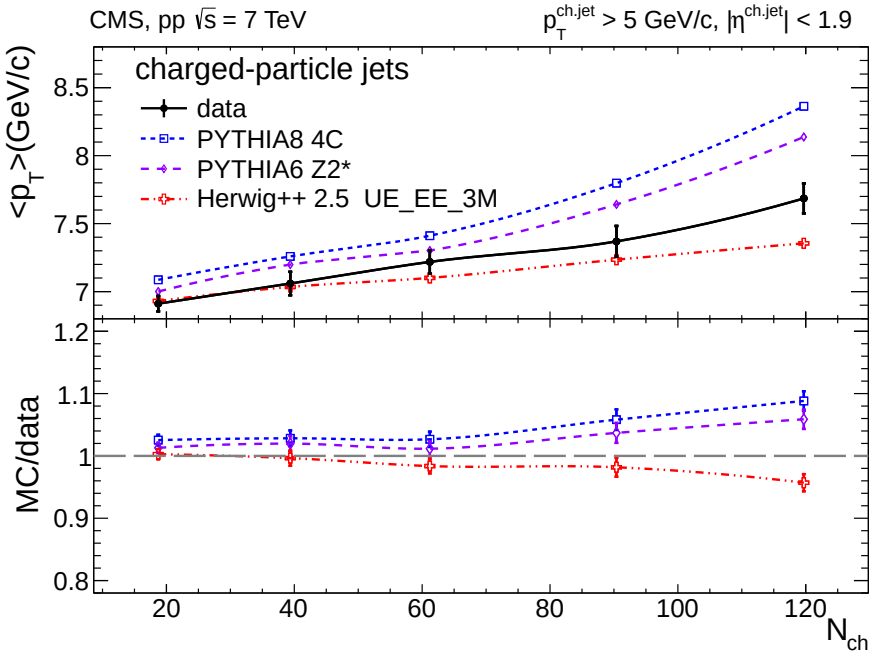

Figure 8: Mean transverse momentum of charged-particle jets with $p_{\mathrm{T}}^{\text{ch. jet}} > 5\,\mathrm{GeV}/c$ and jet axes within $|\eta| < 1.9$) versus charged-particle multiplicity (N_{ch} within $|\eta| < 2.4$) measured in the data (solid line and marker) compared to various MC predictions (non-solid curves and markers). Error bars denote the total uncertainties.

8.2.2 Charged-particle jet spectra

A more detailed picture of the properties of jet spectra both in data and MC simulations is provided by directly comparing the p_{T}-differential distributions in each of the five multiplicity bins shown in Figs. 9–13. In the first three N_{ch} bins the measured jet p_{T} spectra are reasonably well reproduced by the MC predictions. However, in the two highest-multiplicity bins, $80 < N_{\mathrm{ch}} \leq 110$ (Fig. 12) and $110 < N_{\mathrm{ch}} \leq 140$ (Fig. 13), we observe much softer jet spectra for transverse momenta $p_{\mathrm{T}} > 20\,\mathrm{GeV}/c$, where data are lower by a factor of $\sim$2 with respect to PYTHIA predictions. At the same time, HERWIG ++ 2.5 shows the opposite trend, and predicts softer charged-particle jets than measured in data in all multiplicity bins. The relative "softening" of the measured jet spectra compared to PYTHIA at high-N_{ch}, explains also the higher sphericity of high-multiplicity events observed in Ref. [15].

8.2.3 Charged-particle jet widths

The jet width provides important information for characterizing the internal jet radiation dynamics. In this analysis, we quantitatively study the jet width through the p_{T} charged-particle density in ring zones with respect to the jet center, defined as:

$$\rho = \left\langle \frac{1}{p_{\mathrm{T}}^{\text{ch. jet}}} \frac{\delta p_{\mathrm{T}}^{\text{ch. particles}}}{\delta R} \right\rangle_{\text{ch. jets}}, \tag{3}$$

where $R = \sqrt{(\phi - \phi_{\mathrm{jet}})^2 + (\eta - \eta_{\mathrm{jet}})^2}$ is the distance of each charged particle from the jet axis. Larger values of $\rho(R)$ denote a larger transverse momentum fraction in a particular annulus. Jets with $p_{\mathrm{T}}^{\text{ch. jet}} \geq 5\,\mathrm{GeV}/c$ are selected for the study. Data are compared with MC predictions

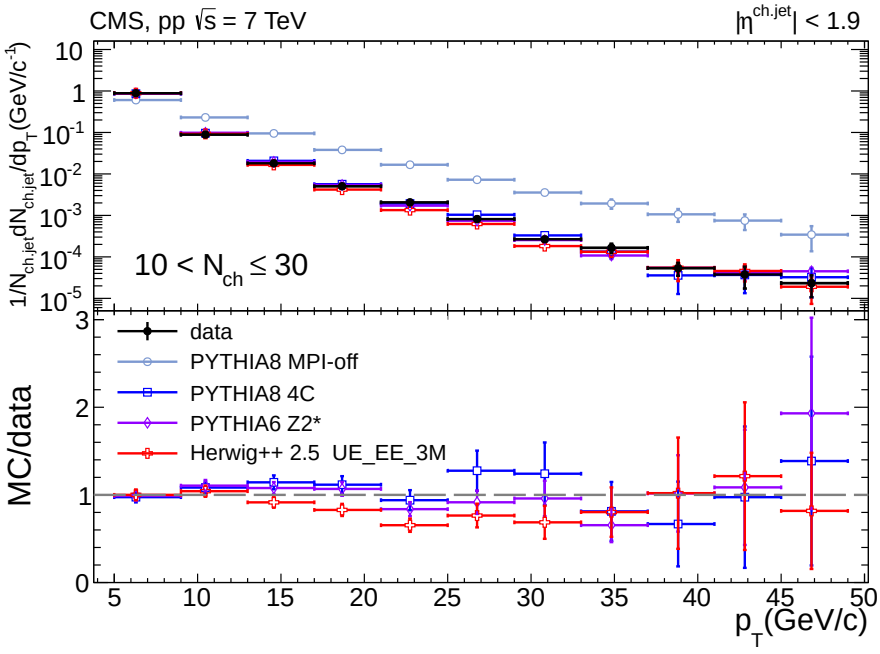

Figure 9: Inclusive charged-particle jet p_{T} spectrum for events with $10 < N_{\mathrm{ch}}(|\eta| < 2.4) \leq 30$ measured in the data (solid dots) compared to various MC predictions (empty markers). Error bars denote the total uncertainties.

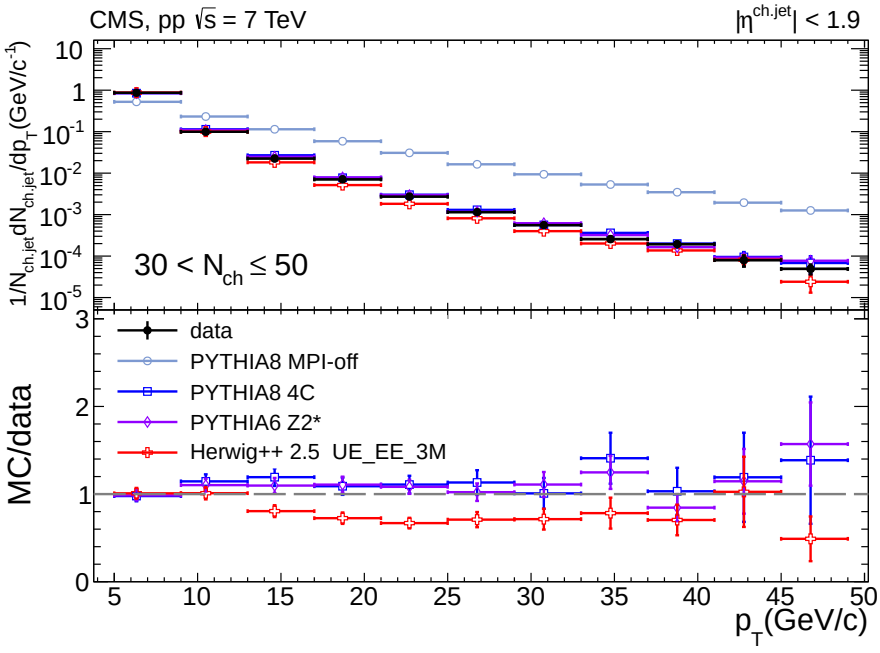

Figure 10: Inclusive charged-particle jet p_{T} spectrum for events with $30 < N_{\mathrm{ch}}(|\eta| < 2.4) \leq 50$ measured in the data (solid dots) compared to various MC predictions (empty markers). Error bars denote the total uncertainties.

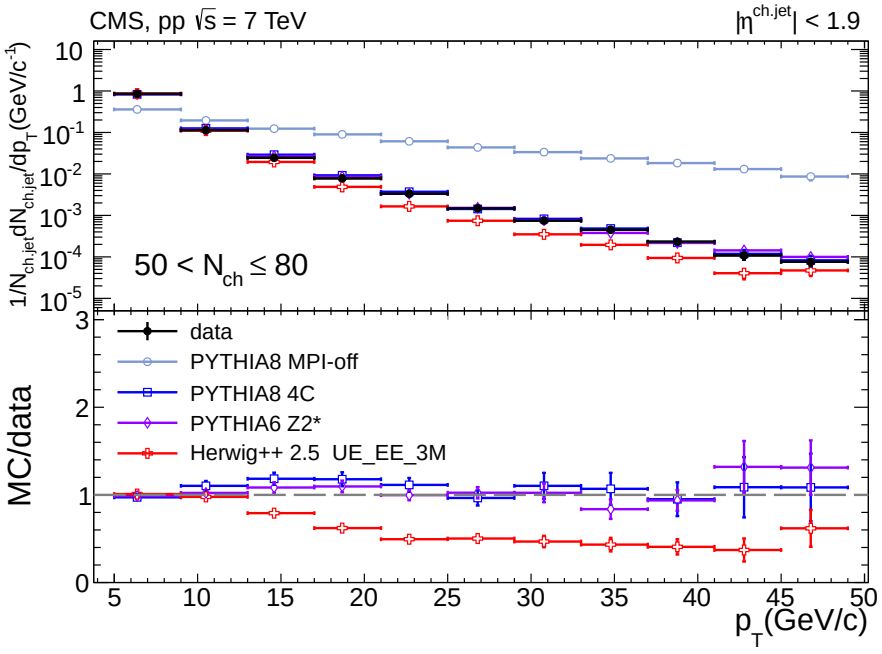

Figure 11: Inclusive charged-particle jet p_{T} spectrum for events with $50 < N_{\mathrm{ch}}(|\eta| < 2.4) \leq 80$ measured in the data (solid dots) compared to various MC predictions (empty markers). Error bars denote the total uncertainties.

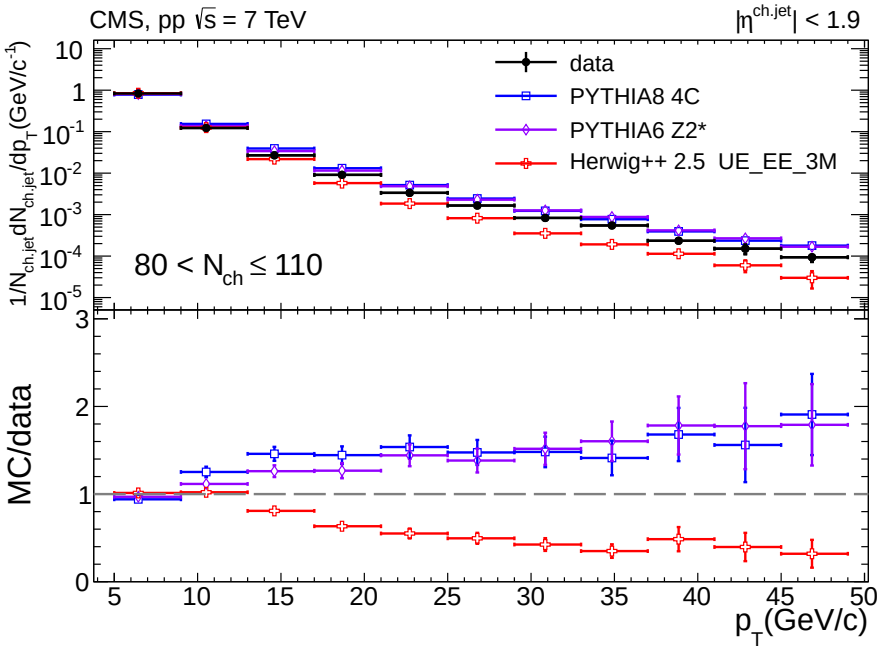

Figure 12: Inclusive charged-particle jet p_{T} spectrum for events with $80 < N_{\mathrm{ch}}(|\eta| < 2.4) \leq 110$ measured in the data (solid dots) compared to various MC predictions (empty markers). Error bars denote the total uncertainties.

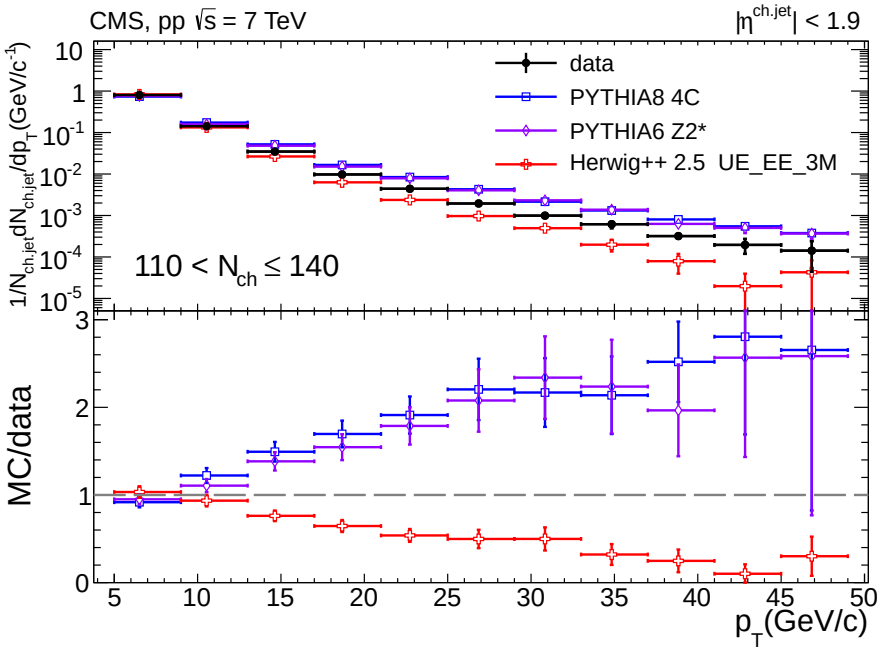

Figure 13: Inclusive charged-particle jet p_{T} spectrum for events with $110 < N_{\mathrm{ch}}(|\eta| < 2.4) \leq 140$ measured in the data (solid dots) compared to various MC predictions (empty markers). Error bars denote the total uncertainties.

in five multiplicity intervals as shown in Figs. 14–18. The dependencies shown in Figs. 14–18 indicate that the jet width increases with N_{ch}, which can be partly explained by the larger contribution of the UE to jets when N_{ch} increases and partly by softer, consequently larger-angle, hadronization, which follows from the intrinsic bias introduced by the requirement of very large values of N_{ch}. In low-multiplicity events, jets are narrower than predicted by PYTHIA and HERWIG, whereas in high-multiplicity events they are of comparable width as predicted by the MC event generators. For events with $10 < N_{\mathrm{ch}} \leq 50$, the PYTHIA 8 model with MPI switched-off shows jet widths that are close to the ones predicted by the models that include MPI, but it produces too hard jets, which are very collimated, in the bin $50 < N_{\mathrm{ch}} \leq 80$. The patterns observed in the data show that the models need to be readjusted to reproduce the activity in the innermost ring zone of the jet as a function of event multiplicity.

9 Conclusions

The characteristics of particle production in pp collisions at $\sqrt{s} = 7$ TeV have been presented as a function of the event charged-particle multiplicity (N_{ch}) by separating the measured charged particles into those belonging to jets and those belonging to the underlying event. Charged particles are measured within the pseudorapidity range $|\eta| < 2.4$ for transverse momenta $p_{\mathrm{T}} > 0.25\,\mathrm{GeV}/c$ and charged-particle jets are reconstructed with $p_{\mathrm{T}} > 5\,\mathrm{GeV}/c$ with charged-particle information only. The distributions of jet p_{T}, average p_{T} of UE charged-particles and jets, jet rates, and jet shapes have been studied as functions of N_{ch} and compared to the predictions of the PYTHIA and HERWIG event generators.

The average trends observed in the data are described by the QCD event generators but the quantitative agreement, in particular at the highest multiplicity, is not as good. The mean transverse momentum of inclusive and UE charged-particles and charged-jets, as well as the

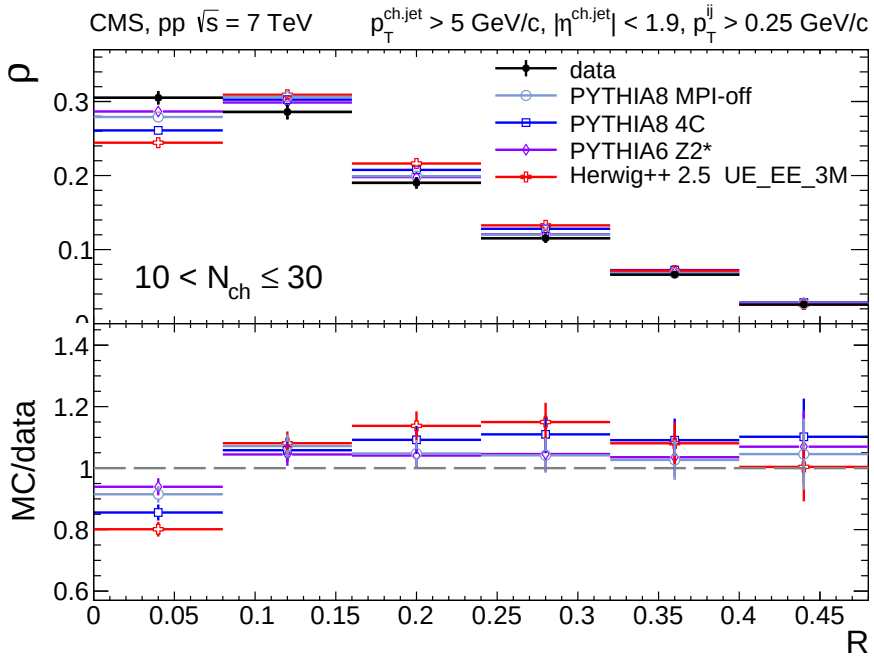

Figure 14: Normalized charged-particle jet p_{T} density ρ in ring zones as a function of distance to the jet axis R for events with $10 < N_{\mathrm{ch}}(|\eta| < 2.4) \leq 30$ measured in the data (solid dots) compared to various MC predictions (empty markers). Error bars denote the total uncertainties.

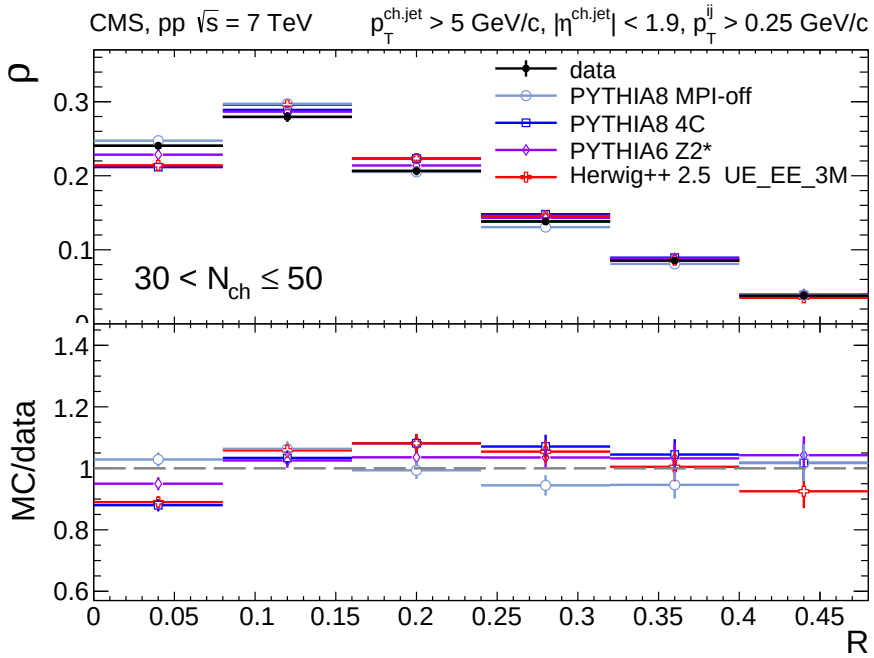

Figure 15: Normalized charged-particle jet p_{T} density ρ in ring zones as a function of distance to the jet axis R for events with $30 < N_{\mathrm{ch}}(|\eta| < 2.4) \leq 50$ measured in the data (solid dots) compared to various MC predictions (empty markers). Error bars denote the total uncertainties.

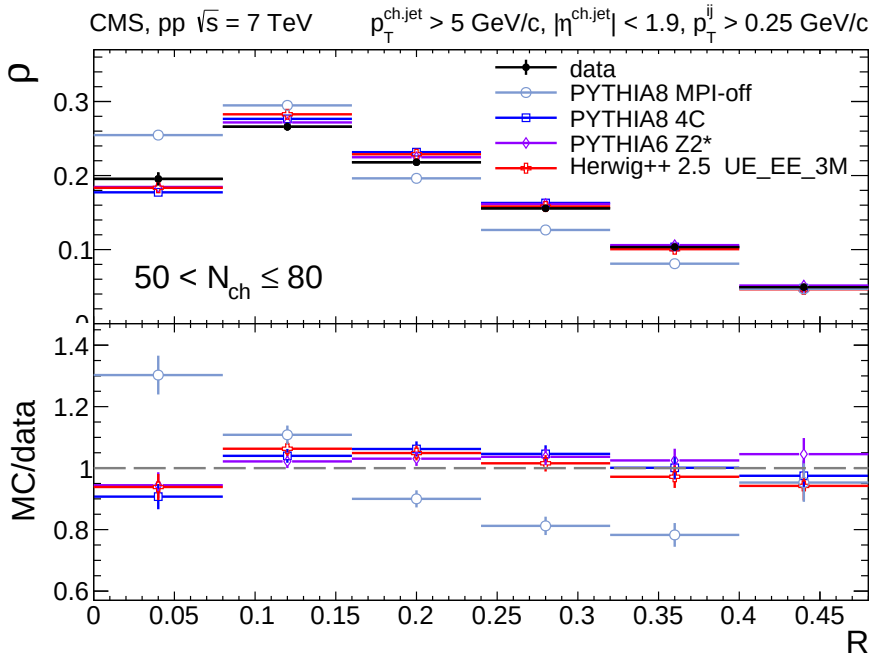

Figure 16: Normalized charged-particle jet p_{T} density ρ in ring zones as a function of distance to the jet axis R for events with $50 < N_{\mathrm{ch}}(|\eta| < 2.4) \leq 80$ measured in the data (solid dots) compared to various MC predictions (empty markers). Error bars denote the total uncertainties.

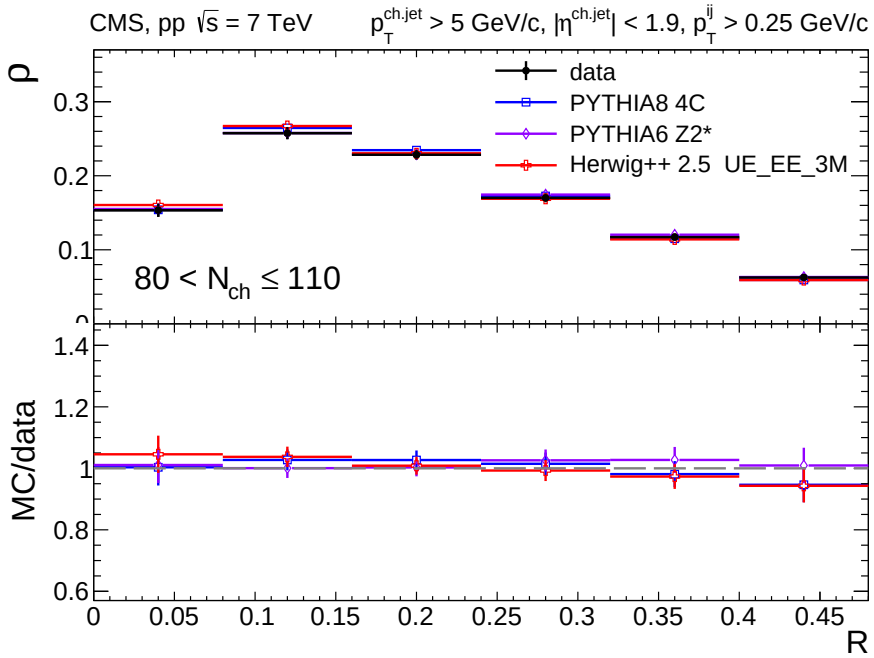

Figure 17: Normalized charged-particle jet p_{T} density ρ in ring zones as a function of distance to the jet axis R for events with $80 < N_{\mathrm{ch}}(|\eta| < 2.4) \leq 110$ measured in the data (solid dots) compared to various MC predictions (empty markers). Error bars denote the total uncertainties.

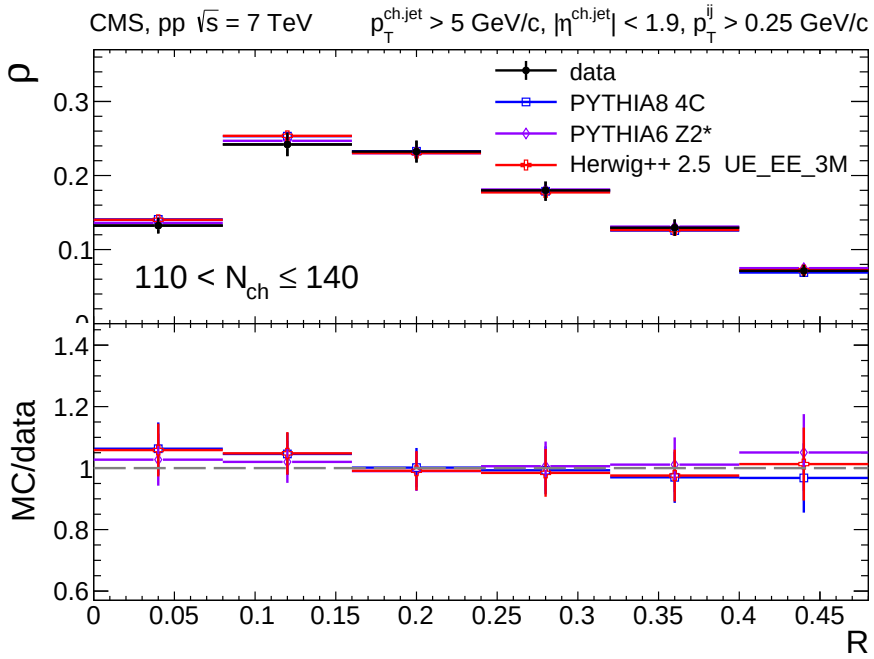

Figure 18: Normalized charged-particle jet p_{T} density ρ in ring zones as a function of distance to the jet axis R for events with $110 < N_{\mathrm{ch}}(|\eta| < 2.4) \leq 140$ measured in the data (solid dots) compared to various MC predictions (empty markers). Error bars denote the total uncertainties.

charged-jet rates, all rise with N_{ch} as expected for an increased fraction of (harder) multiple parton scatterings in more central pp collisions resulting in increasingly higher multiplicity. On the other hand, the average p_{T} of the intrajet constituents and the leading charged-particle of the jets decrease (logarithmically) with increasing N_{ch} as a result of a selection bias: final states with a larger number of hadrons result from (mini)jets which fragment into more, and thus softer, hadrons. The characteristics of the highest multiplicity pp events result from two seemingly opposite trends: a large number of parton interactions with increasingly harder (mini)jets, combined with an overall softer distribution of final-state hadrons.

The detailed features of the N_{ch}-dependence of the jet and the UE properties differ from the MC predictions. In general, PYTHIA (and in particular PYTHIA 6 tune Z2*) reproduces the data better than HERWIG for all observables measured. Of special interest is the large difference between the measured jet p_{T}-differential spectra and the simulation predictions for the highest-multiplicity bins, above N_{ch}=80. In these bins jets are softer, and less abundant than predicted by PYTHIA, which explains the observed larger event sphericity compared to predictions [15]. The MC models also fail to fully describe the intrajet spectra. The deviation of simulation predictions from the data for the spectra of the leading intrajet particle is small in comparison to the variation between different models and their tunes, but systematic. In low-multiplicity events, jets are narrower than predicted by PYTHIA and HERWIG, whereas in high-multiplicity events their widths are as predicted by the MC event generators. At the same time, the characteristics of the UE are well reproduced by most of the MC event generators in all the multiplicity bins considered.

The results obtained in this study are of importance both for improving the MC description of the data and for getting a firmer grasp on the fundamental mechanisms of multi-particle production in hadronic collisions at LHC energies. Current event generators tuned to reproduce

the inelastic LHC data cannot describe within a single approach the dependence of various quantities on event multiplicity. This is especially true in the high-multiplicity range, where PYTHIA produces many particles because of increased high-p_{T} jet contribution and HERWIG++ seems to contain too many soft-parton scatterings. The results of PYTHIA with MPI switched off, demonstrate that the MPI mechanism is critical for reproducing the measured properties of the jets and UE for moderate and large charged-particle multiplicities. Taken together, the MC predictions globally bracket the data and indicate possible ways for improving the parameter tuning and/or including new model ingredients.

Acknowledgments

We congratulate our colleagues in the CERN accelerator departments for the excellent performance of the LHC and thank the technical and administrative staffs at CERN and at other CMS institutes for their contributions to the success of the CMS effort. In addition, we gratefully acknowledge the computing centres and personnel of the Worldwide LHC Computing Grid for delivering so effectively the computing infrastructure essential to our analyses. Finally, we acknowledge the enduring support for the construction and operation of the LHC and the CMS detector provided by the following funding agencies: BMWF and FWF (Austria); FNRS and FWO (Belgium); CNPq, CAPES, FAPERJ, and FAPESP (Brazil); MES (Bulgaria); CERN; CAS, MoST, and NSFC (China); COLCIENCIAS (Colombia); MSES (Croatia); RPF (Cyprus); MoER, SF0690030s09 and ERDF (Estonia); Academy of Finland, MEC, and HIP (Finland); CEA and CNRS/IN2P3 (France); BMBF, DFG, and HGF (Germany); GSRT (Greece); OTKA and NKTH (Hungary); DAE and DST (India); IPM (Iran); SFI (Ireland); INFN (Italy); NRF and WCU (Republic of Korea); LAS (Lithuania); CINVESTAV, CONACYT, SEP, and UASLP-FAI (Mexico); MSI (New Zealand); PAEC (Pakistan); MSHE and NSC (Poland); FCT (Portugal); JINR (Dubna); MON, RosAtom, RAS and RFBR (Russia); MESTD (Serbia); SEIDI and CPAN (Spain); Swiss Funding Agencies (Switzerland); NSC (Taipei); ThEPCenter, IPST, STAR and NSTDA (Thailand); TUBITAK and TAEK (Turkey); NASU (Ukraine); STFC (United Kingdom); DOE and NSF (USA).

Individuals have received support from the Marie-Curie programme and the European Research Council and EPLANET (European Union); the Leventis Foundation; the A. P. Sloan Foundation; the Alexander von Humboldt Foundation; the Belgian Federal Science Policy Office; the Fonds pour la Formation á la Recherche dans l'Industrie et dans l'Agriculture (FRIA-Belgium); the Agentschap voor Innovatie door Wetenschap en Technologie (IWT-Belgium); the Ministry of Education, Youth and Sports (MEYS) of Czech Republic; the Council of Science and Industrial Research, India; the Compagnia di San Paolo (Torino); the HOMING PLUS programme of Foundation for Polish Science, cofinanced by EU, Regional Development Fund; and the Thalis and Aristeia programmes cofinanced by EU-ESF and the Greek NSRF.

References

[1] Yu. L. Dokshitzer, V. A. Khoze, A. H. Mueller, and S. I. Troyan, "Basics of Perturbative QCD". Editions Frontières, 1991.

[2] G. Andersson, G. Gustaffson, G. Ingelman, and T. Sjöstrand, "Parton fragmentation and string dynamics", *Phys. Rept.* **97** (1983) 31, doi:10.1016/0370-1573(83)90080-7.

[3] P. Bartalini and L. Fanò, eds., "Proceedings of the First International Workshop on Multiple Partonic Interactions (MPI '08)". Perugia, Italy, (2008). arXiv:1003.4220.

[4] V. P. Shelest, A. M. Snigirev, and G. M. Zinovjev, "Gazing into the multiparton distribution equations in QCD", *Phys. Lett. B* **113** (1982) 325, doi:10.1016/0370-2693(82)90049-1.

[5] T. Sjöstrand and M. van Zijl, "A multiple-interaction model for the event structure in hadron collisions", *Phys. Rev. D* **36** (1987) 2019, doi:10.1103/PhysRevD.36.2019.

[6] I. M. Dremin and V. A. Nechitailo, "Soft multiple parton interactions as seen in multiplicity distributions at Tevatron and LHC", *Phys. Rev. D* **84** (2011) 034026, doi:10.1103/PhysRevD.84.034026.

[7] M. Diehl, D. Ostermeier, and A. Schäfer, "Elements of a theory for mutiparton interactions in QCD", *JHEP* **03** (2012) 089, doi:10.1007/JHEP03(2012)089.

[8] B. Blok, Yu. Dokshitzer, L. Frankfurt, M. Strikman, "pQCD physics of multiparton interactions", *Eur. Phys. J. C* **72** (2012) 1963, doi:10.1140/epjc/s10052-012-1963-8.

[9] T. Sjöstrand, S. Mrenna, and P. Skands, "PYTHIA 6.4 physics and manual", *JHEP* **05** (2006) 026, doi:10.1088/1126-6708/2006/05/026.

[10] T. Sjöstrand, S. Mrenna, and P. Skands, "A brief introduction to PYTHIA 8.1", *Comput. Phys. Commun.* **178** (2008) 852, doi:10.1016/j.cpc.2008.01.036.

[11] M. Bähr et al., "Herwig++ physics and manual", *Eur. Phys. J. C* **58** (2008) 639, doi:10.1140/epjc/s10052-008-0798-9.

[12] S. Gieseke et al., "Herwig++ 2.5 Release Note", (2011). arXiv:1102.1672.

[13] CMS Collaboration, "Charged particle multiplicities in pp interactions at $\sqrt{s}$ = 0.9, 2.36 and 7 TeV", *JHEP* **01** (2011) 079, doi:10.1007/JHEP01(2011)079.

[14] CMS Collaboration, "Observation of long-range, near-side angular correlations in proton-proton collisions at the LHC", *JHEP* **09** (2010) 091, doi:10.1007/JHEP09(2010)091.

[15] ALICE Collaboration, "Transverse sphericity of primary charged particles in minimum bias proton-proton collisions at $\sqrt{s}$ = 0.9, 2.76 and 7 TeV", *Eur. Phys. J. C* **72** (2012) 2124, doi:10.1140/epjc/s10052-012-2124-9.

[16] ATLAS Collaboration, "Measurement of charged-particle event shape variables in $\sqrt{s}$ = 7 TeV proton-proton interactions with the ATLAS detector", *Phys. Rev. D* **88** (2013) 032004, doi:10.1103/PhysRevD.88.032004.

[17] CMS Collaboration, "First measurement of hadronic event shapes in pp collisions at $\sqrt{s}$ = 7 TeV", *Phys. Lett. B* **699** (2011) 48, doi:10.1016/j.physletb.2011.03.060.

[18] UA1 Collaboration, "A study of the general characteristics of $p\bar{p}$ collisions at $\sqrt{s}$ = 0.2 TeV to 0.9 TeV", *Nucl. Phys. B* **335** (1990) 261, doi:10.1016/0550-3213(90)90493-W.

[19] CDF Collaboration, "Soft and hard interactions in $p\bar{p}$ collisions at $\sqrt{s}$ = 1800 GeV and 630 GeV", *Phys. Rev. D* **65** (2002) 072005, doi:10.1103/PhysRevD.65.072005.

[20] CDF Collaboration, "Measurement of particle production and inclusive differential cross sections in $p\bar{p}$ collisions at $\sqrt{s}$ = 1.96 TeV", *Phys. Rev. D* **79** (2009) 112005, doi:10.1103/PhysRevD.79.112005. Also erratum: doi:10.1103/PhysRevD.82.119903.

[21] ATLAS Collaboration, "Charged-particle multiplicities in pp interactions measured with the ATLAS detector at the LHC", *New J. Phys.* **13** (2011) 053033, doi:10.1088/1367-2630/13/5/053033.

[22] ALICE Collaboration, "Transverse momentum spectra of charged particles in proton-proton collisions at $\sqrt{s} = 900$ GeV with ALICE at the LHC", *Phys. Lett. B* **693** (2010) 53, doi:10.1016/j.physletb.2010.08.026.

[23] CMS Collaboration, "Dependence on pseudorapidity and on centrality of charged hadron production in PbPb collisions at $\sqrt{s_{\mathrm{NN}}}$ = 2.76 TeV", *JHEP* **08** (2011) 141, doi:10.1007/JHEP08(2011)141.

[24] M. Cacciari, G. P. Salam, and G. Soyez, "The anti-k_t jet clustering algorithm", *JHEP* **04** (2008) 063, doi:10.1088/1126-6708/2008/04/063.

[25] M. Cacciari, G. P. Salam, and G. Soyez, "FastJet user manual", *Eur. Phys. J. C* **72** (2012) 1896, doi:10.1140/epjc/s10052-012-1896-2.

[26] CMS Collaboration, "The CMS experiment at the CERN LHC", *JINST* **3** (2008) S08004, doi:10.1088/1748-0221/3/08/S08004.

[27] R. Corke and T. Sjöstrand, "Interleaved parton showers and tuning prospects", *JHEP* **03** (2011) 032, doi:10.1007/JHEP03(2011)032.

[28] A. Leonidov, "On transverse energy production in hadron collisions", (2000). arXiv:hep-ph/0005010.

[29] P. Z. Skands and D. Wicke, "Non-perturbative QCD effects and the top mass at the Tevatron", *Eur. Phys. J. C* **52** (2007) 133, doi:10.1140/epjc/s10052-007-0352-1.

[30] A. Buckley et al., "General-purpose event generators for LHC physics", *Phys. Rept.* **504** (2011) 145, doi:10.1016/j.physrep.2011.03.005.

[31] R. Field, "Early LHC underlying event data—Findings and surprises", in *Hadron Collider Physics Symposium 2010 (HCP2010)*. Toronto, Canada, 2010. arXiv:1010.3558.

[32] J. Pumplin et al., "New generation of parton distributions with uncertainties from global QCD analysis", *JHEP* **07** (2002) 012, doi:10.1088/1126-6708/2002/07/012.

[33] A. Buckley et al., "Systematic event generator tuning for the LHC", *Eur. Phys. J. C* **65** (2010) 331, doi:10.1140/epjc/s10052-009-1196-7.

[34] R. S. Thorne, A. D. Martin, W. J. Stirling, and G. Watt, "Status of MRST/MSTW PDF sets", (2009). arXiv:0907.2387.

[35] CMS Collaboration, "CMS tracking performance results from Early LHC operation", *Eur. Phys. J. C* **70** (2010) 1165, doi:10.1140/epjc/s10052-010-1491-3.

[36] CMS Collaboration, "Track and vertex reconstruction in CMS", *Nucl. Instrum. Meth. A* **582** (2007) 781, doi:10.1016/j.nima.2007.07.091.

[37] G. D'Agostini, "A multidimensional unfolding method based on Bayes' theorem", *Nucl. Instrum. Meth. A* **362** (1995) 487, doi:10.1016/0168-9002(95)00274-X.

[38] CMS Collaboration, "Transverse-momentum and pseudorapidity distributions of charged hadrons in pp collisions at at $\sqrt{s}$ = 0.9 and 2.36 TeV", *JHEP* **02** (2010) 041, doi:10.1007/JHEP02(2010)041.

[39] CMS Collaboration, "Shape, transverse size, and charged hadron multiplicity of jets in pp collisions at $\sqrt{s}$ = 7 TeV", *JHEP* **06** (2012) 160, doi:10.1007/JHEP06(2012)160.

[40] ATLAS Collaboration, "Measurement of event shapes at large momentum transfer with the ATLAS detector in pp collisions at $\sqrt{s}$ = 7 TeV", *Eur. Phys. J. C* **72** (2012) 2211, doi:10.1140/epjc/s10052-012-2211-y.

[41] ATLAS Collaboration, "Study of jet shapes in inclusive jet production in pp collisions at $\sqrt{s}$ = 7 TeV using the ATLAS detector", *Phys. Rev. D* **83** (2011) 052003, doi:10.1103/PhysRevD.83.052003.

A The CMS Collaboration

Yerevan Physics Institute, Yerevan, Armenia
S. Chatrchyan, V. Khachatryan, A.M. Sirunyan, A. Tumasyan

Institut für Hochenergiephysik der OeAW, Wien, Austria
W. Adam, T. Bergauer, M. Dragicevic, J. Erö, C. Fabjan[1], M. Friedl, R. Frühwirth[1], V.M. Ghete, N. Hörmann, J. Hrubec, M. Jeitler[1], W. Kiesenhofer, V. Knünz, M. Krammer[1], I. Krätschmer, D. Liko, I. Mikulec, D. Rabady[2], B. Rahbaran, C. Rohringer, H. Rohringer, R. Schöfbeck, J. Strauss, A. Taurok, W. Treberer-Treberspurg, W. Waltenberger, C.-E. Wulz[1]

National Centre for Particle and High Energy Physics, Minsk, Belarus
V. Mossolov, N. Shumeiko, J. Suarez Gonzalez

Universiteit Antwerpen, Antwerpen, Belgium
S. Alderweireldt, M. Bansal, S. Bansal, T. Cornelis, E.A. De Wolf, X. Janssen, A. Knutsson, S. Luyckx, L. Mucibello, S. Ochesanu, B. Roland, R. Rougny, Z. Staykova, H. Van Haevermaet, P. Van Mechelen, N. Van Remortel, A. Van Spilbeeck

Vrije Universiteit Brussel, Brussel, Belgium
F. Blekman, S. Blyweert, J. D'Hondt, A. Kalogeropoulos, J. Keaveney, S. Lowette, M. Maes, A. Olbrechts, S. Tavernier, W. Van Doninck, P. Van Mulders, G.P. Van Onsem, I. Villella

Université Libre de Bruxelles, Bruxelles, Belgium
C. Caillol, B. Clerbaux, G. De Lentdecker, L. Favart, A.P.R. Gay, T. Hreus, A. Léonard, P.E. Marage, A. Mohammadi, L. Perniè, T. Reis, T. Seva, L. Thomas, C. Vander Velde, P. Vanlaer, J. Wang

Ghent University, Ghent, Belgium
V. Adler, K. Beernaert, L. Benucci, A. Cimmino, S. Costantini, S. Dildick, G. Garcia, B. Klein, J. Lellouch, A. Marinov, J. Mccartin, A.A. Ocampo Rios, D. Ryckbosch, M. Sigamani, N. Strobbe, F. Thyssen, M. Tytgat, S. Walsh, E. Yazgan, N. Zaganidis

Université Catholique de Louvain, Louvain-la-Neuve, Belgium
S. Basegmez, C. Beluffi[3], G. Bruno, R. Castello, A. Caudron, L. Ceard, G.G. Da Silveira, C. Delaere, T. du Pree, D. Favart, L. Forthomme, A. Giammanco[4], J. Hollar, P. Jez, V. Lemaitre, J. Liao, O. Militaru, C. Nuttens, D. Pagano, A. Pin, K. Piotrzkowski, A. Popov[5], M. Selvaggi, M. Vidal Marono, J.M. Vizan Garcia

Université de Mons, Mons, Belgium
N. Beliy, T. Caebergs, E. Daubie, G.H. Hammad

Centro Brasileiro de Pesquisas Fisicas, Rio de Janeiro, Brazil
G.A. Alves, M. Correa Martins Junior, T. Martins, M.E. Pol, M.H.G. Souza

Universidade do Estado do Rio de Janeiro, Rio de Janeiro, Brazil
W.L. Aldá Júnior, W. Carvalho, J. Chinellato[6], A. Custódio, E.M. Da Costa, D. De Jesus Damiao, C. De Oliveira Martins, S. Fonseca De Souza, H. Malbouisson, M. Malek, D. Matos Figueiredo, L. Mundim, H. Nogima, W.L. Prado Da Silva, A. Santoro, A. Sznajder, E.J. Tonelli Manganote[6], A. Vilela Pereira

Universidade Estadual Paulista [a], Universidade Federal do ABC [b], São Paulo, Brazil
C.A. Bernardes[b], F.A. Dias[a,7], T.R. Fernandez Perez Tomei[a], E.M. Gregores[b], C. Lagana[a], P.G. Mercadante[b], S.F. Novaes[a], Sandra S. Padula[a]

Institute for Nuclear Research and Nuclear Energy, Sofia, Bulgaria
V. Genchev[2], P. Iaydjiev[2], S. Piperov, M. Rodozov, G. Sultanov, M. Vutova

University of Sofia, Sofia, Bulgaria
A. Dimitrov, R. Hadjiiska, V. Kozhuharov, L. Litov, B. Pavlov, P. Petkov

Institute of High Energy Physics, Beijing, China
J.G. Bian, G.M. Chen, H.S. Chen, C.H. Jiang, D. Liang, S. Liang, X. Meng, J. Tao, X. Wang, Z. Wang

State Key Laboratory of Nuclear Physics and Technology, Peking University, Beijing, China
C. Asawatangtrakuldee, Y. Ban, Y. Guo, Q. Li, W. Li, S. Liu, Y. Mao, S.J. Qian, D. Wang, L. Zhang, W. Zou

Universidad de Los Andes, Bogota, Colombia
C. Avila, C.A. Carrillo Montoya, L.F. Chaparro Sierra, J.P. Gomez, B. Gomez Moreno, J.C. Sanabria

Technical University of Split, Split, Croatia
N. Godinovic, D. Lelas, R. Plestina[8], D. Polic, I. Puljak

University of Split, Split, Croatia
Z. Antunovic, M. Kovac

Institute Rudjer Boskovic, Zagreb, Croatia
V. Brigljevic, K. Kadija, J. Luetic, D. Mekterovic, S. Morovic, L. Tikvica

University of Cyprus, Nicosia, Cyprus
A. Attikis, G. Mavromanolakis, J. Mousa, C. Nicolaou, F. Ptochos, P.A. Razis

Charles University, Prague, Czech Republic
M. Finger, M. Finger Jr.

Academy of Scientific Research and Technology of the Arab Republic of Egypt, Egyptian Network of High Energy Physics, Cairo, Egypt
A.A. Abdelalim[9], Y. Assran[10], S. Elgammal[9], A. Ellithi Kamel[11], M.A. Mahmoud[12], A. Radi[13,14]

National Institute of Chemical Physics and Biophysics, Tallinn, Estonia
M. Kadastik, M. Müntel, M. Murumaa, M. Raidal, L. Rebane, A. Tiko

Department of Physics, University of Helsinki, Helsinki, Finland
P. Eerola, G. Fedi, M. Voutilainen

Helsinki Institute of Physics, Helsinki, Finland
J. Härkönen, V. Karimäki, R. Kinnunen, M.J. Kortelainen, T. Lampén, K. Lassila-Perini, S. Lehti, T. Lindén, P. Luukka, T. Mäenpää, T. Peltola, E. Tuominen, J. Tuominiemi, E. Tuovinen, L. Wendland

Lappeenranta University of Technology, Lappeenranta, Finland
T. Tuuva

DSM/IRFU, CEA/Saclay, Gif-sur-Yvette, France
M. Besancon, F. Couderc, M. Dejardin, D. Denegri, B. Fabbro, J.L. Faure, F. Ferri, S. Ganjour, A. Givernaud, P. Gras, G. Hamel de Monchenault, P. Jarry, E. Locci, J. Malcles, L. Millischer, A. Nayak, J. Rander, A. Rosowsky, M. Titov

Laboratoire Leprince-Ringuet, Ecole Polytechnique, IN2P3-CNRS, Palaiseau, France
S. Baffioni, F. Beaudette, L. Benhabib, M. Bluj[15], P. Busson, C. Charlot, N. Daci, T. Dahms, M. Dalchenko, L. Dobrzynski, A. Florent, R. Granier de Cassagnac, M. Haguenauer, P. Miné, C. Mironov, I.N. Naranjo, M. Nguyen, C. Ochando, P. Paganini, D. Sabes, R. Salerno, Y. Sirois, C. Veelken, A. Zabi

Institut Pluridisciplinaire Hubert Curien, Université de Strasbourg, Université de Haute Alsace Mulhouse, CNRS/IN2P3, Strasbourg, France
J.-L. Agram[16], J. Andrea, D. Bloch, J.-M. Brom, E.C. Chabert, C. Collard, E. Conte[16], F. Drouhin[16], J.-C. Fontaine[16], D. Gelé, U. Goerlach, C. Goetzmann, P. Juillot, A.-C. Le Bihan, P. Van Hove

Centre de Calcul de l'Institut National de Physique Nucleaire et de Physique des Particules, CNRS/IN2P3, Villeurbanne, France
S. Gadrat

Université de Lyon, Université Claude Bernard Lyon 1, CNRS-IN2P3, Institut de Physique Nucléaire de Lyon, Villeurbanne, France
S. Beauceron, N. Beaupere, G. Boudoul, S. Brochet, J. Chasserat, R. Chierici, D. Contardo, P. Depasse, H. El Mamouni, J. Fan, J. Fay, S. Gascon, M. Gouzevitch, B. Ille, T. Kurca, M. Lethuillier, L. Mirabito, S. Perries, L. Sgandurra, V. Sordini, M. Vander Donckt, P. Verdier, S. Viret, H. Xiao

Institute of High Energy Physics and Informatization, Tbilisi State University, Tbilisi, Georgia
Z. Tsamalaidze[17]

RWTH Aachen University, I. Physikalisches Institut, Aachen, Germany
C. Autermann, S. Beranek, M. Bontenackels, B. Calpas, M. Edelhoff, L. Feld, N. Heracleous, O. Hindrichs, K. Klein, A. Ostapchuk, A. Perieanu, F. Raupach, J. Sammet, S. Schael, D. Sprenger, H. Weber, B. Wittmer, V. Zhukov[5]

RWTH Aachen University, III. Physikalisches Institut A, Aachen, Germany
M. Ata, J. Caudron, E. Dietz-Laursonn, D. Duchardt, M. Erdmann, R. Fischer, A. Güth, T. Hebbeker, C. Heidemann, K. Hoepfner, D. Klingebiel, S. Knutzen, P. Kreuzer, M. Merschmeyer, A. Meyer, M. Olschewski, K. Padeken, P. Papacz, H. Pieta, H. Reithler, S.A. Schmitz, L. Sonnenschein, J. Steggemann, D. Teyssier, S. Thüer, M. Weber

RWTH Aachen University, III. Physikalisches Institut B, Aachen, Germany
V. Cherepanov, Y. Erdogan, G. Flügge, H. Geenen, M. Geisler, W. Haj Ahmad, F. Hoehle, B. Kargoll, T. Kress, Y. Kuessel, J. Lingemann[2], A. Nowack, I.M. Nugent, L. Perchalla, O. Pooth, A. Stahl

Deutsches Elektronen-Synchrotron, Hamburg, Germany
I. Asin, N. Bartosik, J. Behr, W. Behrenhoff, U. Behrens, A.J. Bell, M. Bergholz[18], A. Bethani, K. Borras, A. Burgmeier, A. Cakir, L. Calligaris, A. Campbell, S. Choudhury, F. Costanza, C. Diez Pardos, S. Dooling, T. Dorland, G. Eckerlin, D. Eckstein, G. Flucke, A. Geiser, I. Glushkov, A. Grebenyuk, P. Gunnellini, S. Habib, J. Hauk, G. Hellwig, D. Horton, H. Jung, M. Kasemann, P. Katsas, C. Kleinwort, H. Kluge, M. Krämer, D. Krücker, E. Kuznetsova, W. Lange, J. Leonard, K. Lipka, W. Lohmann[18], B. Lutz, R. Mankel, I. Marfin, I.-A. Melzer-Pellmann, A.B. Meyer, J. Mnich, A. Mussgiller, S. Naumann-Emme, O. Novgorodova, F. Nowak, J. Olzem, H. Perrey, A. Petrukhin, D. Pitzl, R. Placakyte, A. Raspereza, P.M. Ribeiro

Cipriano, C. Riedl, E. Ron, M.Ö. Sahin, J. Salfeld-Nebgen, R. Schmidt[18], T. Schoerner-Sadenius, N. Sen, M. Stein, R. Walsh, C. Wissing

University of Hamburg, Hamburg, Germany
M. Aldaya Martin, V. Blobel, H. Enderle, J. Erfle, E. Garutti, U. Gebbert, M. Görner, M. Gosselink, J. Haller, K. Heine, R.S. Höing, G. Kaussen, H. Kirschenmann, R. Klanner, R. Kogler, J. Lange, I. Marchesini, T. Peiffer, N. Pietsch, D. Rathjens, C. Sander, H. Schettler, P. Schleper, E. Schlieckau, A. Schmidt, M. Schröder, T. Schum, M. Seidel, J. Sibille[19], V. Sola, H. Stadie, G. Steinbrück, J. Thomsen, D. Troendle, E. Usai, L. Vanelderen

Institut für Experimentelle Kernphysik, Karlsruhe, Germany
C. Barth, C. Baus, J. Berger, C. Böser, E. Butz, T. Chwalek, W. De Boer, A. Descroix, A. Dierlamm, M. Feindt, M. Guthoff[2], F. Hartmann[2], T. Hauth[2], H. Held, K.H. Hoffmann, U. Husemann, I. Katkov[5], J.R. Komaragiri, A. Kornmayer[2], P. Lobelle Pardo, D. Martschei, M.U. Mozer, Th. Müller, M. Niegel, A. Nürnberg, O. Oberst, J. Ott, G. Quast, K. Rabbertz, F. Ratnikov, S. Röcker, F.-P. Schilling, G. Schott, H.J. Simonis, F.M. Stober, R. Ulrich, J. Wagner-Kuhr, S. Wayand, T. Weiler, M. Zeise

Institute of Nuclear and Particle Physics (INPP), NCSR Demokritos, Aghia Paraskevi, Greece
G. Anagnostou, G. Daskalakis, T. Geralis, S. Kesisoglou, A. Kyriakis, D. Loukas, A. Markou, C. Markou, E. Ntomari, I. Topsis-giotis

University of Athens, Athens, Greece
L. Gouskos, A. Panagiotou, N. Saoulidou, E. Stiliaris

University of Ioánnina, Ioánnina, Greece
X. Aslanoglou, I. Evangelou, G. Flouris, C. Foudas, P. Kokkas, N. Manthos, I. Papadopoulos, E. Paradas

KFKI Research Institute for Particle and Nuclear Physics, Budapest, Hungary
G. Bencze, C. Hajdu, P. Hidas, D. Horvath[20], F. Sikler, V. Veszpremi, G. Vesztergombi[21], A.J. Zsigmond

Institute of Nuclear Research ATOMKI, Debrecen, Hungary
N. Beni, S. Czellar, J. Molnar, J. Palinkas, Z. Szillasi

University of Debrecen, Debrecen, Hungary
J. Karancsi, P. Raics, Z.L. Trocsanyi, B. Ujvari

National Institute of Science Education and Research, Bhubaneswar, India
S.K. Swain[22]

Panjab University, Chandigarh, India
S.B. Beri, V. Bhatnagar, N. Dhingra, R. Gupta, M. Kaur, M.Z. Mehta, M. Mittal, N. Nishu, A. Sharma, J.B. Singh

University of Delhi, Delhi, India
Ashok Kumar, Arun Kumar, S. Ahuja, A. Bhardwaj, B.C. Choudhary, A. Kumar, S. Malhotra, M. Naimuddin, K. Ranjan, P. Saxena, V. Sharma, R.K. Shivpuri

Saha Institute of Nuclear Physics, Kolkata, India
S. Banerjee, S. Bhattacharya, K. Chatterjee, S. Dutta, B. Gomber, Sa. Jain, Sh. Jain, R. Khurana, A. Modak, S. Mukherjee, D. Roy, S. Sarkar, M. Sharan, A.P. Singh

Bhabha Atomic Research Centre, Mumbai, India
A. Abdulsalam, D. Dutta, S. Kailas, V. Kumar, A.K. Mohanty[2], L.M. Pant, P. Shukla, A. Topkar

Tata Institute of Fundamental Research - EHEP, Mumbai, India
T. Aziz, R.M. Chatterjee, S. Ganguly, S. Ghosh, M. Guchait[23], A. Gurtu[24], G. Kole, S. Kumar, M. Maity[25], G. Majumder, K. Mazumdar, G.B. Mohanty, B. Parida, K. Sudhakar, N. Wickramage[26]

Tata Institute of Fundamental Research - HECR, Mumbai, India
S. Banerjee, S. Dugad

Institute for Research in Fundamental Sciences (IPM), Tehran, Iran
H. Arfaei, H. Bakhshiansohi, S.M. Etesami[27], A. Fahim[28], A. Jafari, M. Khakzad, M. Mohammadi Najafabadi, S. Paktinat Mehdiabadi, B. Safarzadeh[29], M. Zeinali

University College Dublin, Dublin, Ireland
M. Grunewald

INFN Sezione di Bari [a], Università di Bari [b], Politecnico di Bari [c], Bari, Italy
M. Abbrescia[a,b], L. Barbone[a,b], C. Calabria[a,b], S.S. Chhibra[a,b], A. Colaleo[a], D. Creanza[a,c], N. De Filippis[a,c], M. De Palma[a,b], L. Fiore[a], G. Iaselli[a,c], G. Maggi[a,c], M. Maggi[a], B. Marangelli[a,b], S. My[a,c], S. Nuzzo[a,b], N. Pacifico[a], A. Pompili[a,b], G. Pugliese[a,c], G. Selvaggi[a,b], L. Silvestris[a], G. Singh[a,b], R. Venditti[a,b], P. Verwilligen[a], G. Zito[a]

INFN Sezione di Bologna [a], Università di Bologna [b], Bologna, Italy
G. Abbiendi[a], A.C. Benvenuti[a], D. Bonacorsi[a,b], S. Braibant-Giacomelli[a,b], L. Brigliadori[a,b], R. Campanini[a,b], P. Capiluppi[a,b], A. Castro[a,b], F.R. Cavallo[a], G. Codispoti[a,b], M. Cuffiani[a,b], G.M. Dallavalle[a], F. Fabbri[a], A. Fanfani[a,b], D. Fasanella[a,b], P. Giacomelli[a], C. Grandi[a], L. Guiducci[a,b], S. Marcellini[a], G. Masetti[a], M. Meneghelli[a,b], A. Montanari[a], F.L. Navarria[a,b], F. Odorici[a], A. Perrotta[a], F. Primavera[a,b], A.M. Rossi[a,b], T. Rovelli[a,b], G.P. Siroli[a,b], N. Tosi[a,b], R. Travaglini[a,b]

INFN Sezione di Catania [a], Università di Catania [b], Catania, Italy
S. Albergo[a,b], M. Chiorboli[a,b], S. Costa[a,b], F. Giordano[a,2], R. Potenza[a,b], A. Tricomi[a,b], C. Tuve[a,b]

INFN Sezione di Firenze [a], Università di Firenze [b], Firenze, Italy
G. Barbagli[a], V. Ciulli[a,b], C. Civinini[a], R. D'Alessandro[a,b], E. Focardi[a,b], S. Frosali[a,b], E. Gallo[a], S. Gonzi[a,b], V. Gori[a,b], P. Lenzi[a,b], M. Meschini[a], S. Paoletti[a], G. Sguazzoni[a], A. Tropiano[a,b]

INFN Laboratori Nazionali di Frascati, Frascati, Italy
L. Benussi, S. Bianco, F. Fabbri, D. Piccolo

INFN Sezione di Genova [a], Università di Genova [b], Genova, Italy
P. Fabbricatore[a], R. Ferretti[a,b], F. Ferro[a], M. Lo Vetere[a,b], R. Musenich[a], E. Robutti[a], S. Tosi[a,b]

INFN Sezione di Milano-Bicocca [a], Università di Milano-Bicocca [b], Milano, Italy
A. Benaglia[a], M.E. Dinardo[a,b], S. Fiorendi[a,b], S. Gennai[a], A. Ghezzi[a,b], P. Govoni[a,b], M.T. Lucchini[a,b,2], S. Malvezzi[a], R.A. Manzoni[a,b,2], A. Martelli[a,b,2], D. Menasce[a], L. Moroni[a], M. Paganoni[a,b], D. Pedrini[a], S. Ragazzi[a,b], N. Redaelli[a], T. Tabarelli de Fatis[a,b]

INFN Sezione di Napoli [a], Università di Napoli 'Federico II' [b], Università della Basilicata (Potenza) [c], Università G. Marconi (Roma) [d], Napoli, Italy
S. Buontempo[a], N. Cavallo[a,c], A. De Cosa[a,b], F. Fabozzi[a,c], A.O.M. Iorio[a,b], L. Lista[a], S. Meola[a,d,2], M. Merola[a], P. Paolucci[a,2]

INFN Sezione di Padova [a], Università di Padova [b], Università di Trento (Trento) [c], Padova, Italy
P. Azzi[a], N. Bacchetta[a], M. Bellato[a], D. Bisello[a,b], A. Branca[a,b], R. Carlin[a,b], P. Checchia[a], T. Dorigo[a], F. Fanzago[a], M. Galanti[a,b,2], F. Gasparini[a,b], U. Gasparini[a,b], P. Giubilato[a,b], A. Gozzelino[a], K. Kanishchev[a,c], S. Lacaprara[a], I. Lazzizzera[a,c], M. Margoni[a,b], A.T. Meneguzzo[a,b], M. Passaseo[a], J. Pazzini[a,b], M. Pegoraro[a], N. Pozzobon[a,b], P. Ronchese[a,b], F. Simonetto[a,b], E. Torassa[a], M. Tosi[a,b], S. Vanini[a,b], P. Zotto[a,b], A. Zucchetta[a,b], G. Zumerle[a,b]

INFN Sezione di Pavia [a], Università di Pavia [b], Pavia, Italy
M. Gabusi[a,b], S.P. Ratti[a,b], C. Riccardi[a,b], P. Vitulo[a,b]

INFN Sezione di Perugia [a], Università di Perugia [b], Perugia, Italy
M. Biasini[a,b], G.M. Bilei[a], L. Fanò[a,b], P. Lariccia[a,b], G. Mantovani[a,b], M. Menichelli[a], A. Nappi[a,b†], F. Romeo[a,b], A. Saha[a], A. Santocchia[a,b], A. Spiezia[a,b]

INFN Sezione di Pisa [a], Università di Pisa [b], Scuola Normale Superiore di Pisa [c], Pisa, Italy
K. Androsov[a,30], P. Azzurri[a], G. Bagliesi[a], J. Bernardini[a], T. Boccali[a], G. Broccolo[a,c], R. Castaldi[a], M.A. Ciocci[a], R.T. D'Agnolo[a,c,2], R. Dell'Orso[a], F. Fiori[a,c], L. Foà[a,c], A. Giassi[a], M.T. Grippo[a,30], A. Kraan[a], F. Ligabue[a,c], T. Lomtadze[a], L. Martini[a,30], A. Messineo[a,b], C.S. Moon[a], F. Palla[a], A. Rizzi[a,b], A. Savoy-Navarro[a,31], A.T. Serban[a], P. Spagnolo[a], P. Squillacioti[a], R. Tenchini[a], G. Tonelli[a,b], A. Venturi[a], P.G. Verdini[a], C. Vernieri[a,c]

INFN Sezione di Roma [a], Università di Roma [b], Roma, Italy
L. Barone[a,b], F. Cavallari[a], D. Del Re[a,b], M. Diemoz[a], M. Grassi[a,b], E. Longo[a,b], F. Margaroli[a,b], P. Meridiani[a], F. Micheli[a,b], S. Nourbakhsh[a,b], G. Organtini[a,b], R. Paramatti[a], S. Rahatlou[a,b], C. Rovelli[a], L. Soffi[a,b]

INFN Sezione di Torino [a], Università di Torino [b], Università del Piemonte Orientale (Novara) [c], Torino, Italy
N. Amapane[a,b], R. Arcidiacono[a,c], S. Argiro[a,b], M. Arneodo[a,c], R. Bellan[a,b], C. Biino[a], N. Cartiglia[a], S. Casasso[a,b], M. Costa[a,b], A. Degano[a,b], N. Demaria[a], C. Mariotti[a], S. Maselli[a], E. Migliore[a,b], V. Monaco[a,b], M. Musich[a], M.M. Obertino[a,c], N. Pastrone[a], M. Pelliccioni[a,2], A. Potenza[a,b], A. Romero[a,b], M. Ruspa[a,c], R. Sacchi[a,b], A. Solano[a,b], A. Staiano[a], U. Tamponi[a]

INFN Sezione di Trieste [a], Università di Trieste [b], Trieste, Italy
S. Belforte[a], V. Candelise[a,b], M. Casarsa[a], F. Cossutti[a,2], G. Della Ricca[a,b], B. Gobbo[a], C. La Licata[a,b], M. Marone[a,b], D. Montanino[a,b], A. Penzo[a], A. Schizzi[a,b], A. Zanetti[a]

Kangwon National University, Chunchon, Korea
S. Chang, T.Y. Kim, S.K. Nam

Kyungpook National University, Daegu, Korea
D.H. Kim, G.N. Kim, J.E. Kim, D.J. Kong, S. Lee, Y.D. Oh, H. Park, D.C. Son

Chonnam National University, Institute for Universe and Elementary Particles, Kwangju, Korea
J.Y. Kim, Zero J. Kim, S. Song

Korea University, Seoul, Korea
S. Choi, D. Gyun, B. Hong, M. Jo, H. Kim, T.J. Kim, K.S. Lee, S.K. Park, Y. Roh

University of Seoul, Seoul, Korea
M. Choi, J.H. Kim, C. Park, I.C. Park, S. Park, G. Ryu

Sungkyunkwan University, Suwon, Korea
Y. Choi, Y.K. Choi, J. Goh, M.S. Kim, E. Kwon, B. Lee, J. Lee, S. Lee, H. Seo, I. Yu

Vilnius University, Vilnius, Lithuania
I. Grigelionis, A. Juodagalvis

Centro de Investigacion y de Estudios Avanzados del IPN, Mexico City, Mexico
H. Castilla-Valdez, E. De La Cruz-Burelo, I. Heredia-de La Cruz[32], R. Lopez-Fernandez, J. Martínez-Ortega, A. Sanchez-Hernandez, L.M. Villasenor-Cendejas

Universidad Iberoamericana, Mexico City, Mexico
S. Carrillo Moreno, F. Vazquez Valencia

Benemerita Universidad Autonoma de Puebla, Puebla, Mexico
H.A. Salazar Ibarguen

Universidad Autónoma de San Luis Potosí, San Luis Potosí, Mexico
E. Casimiro Linares, A. Morelos Pineda, M.A. Reyes-Santos

University of Auckland, Auckland, New Zealand
D. Krofcheck

University of Canterbury, Christchurch, New Zealand
P.H. Butler, R. Doesburg, S. Reucroft, H. Silverwood

National Centre for Physics, Quaid-I-Azam University, Islamabad, Pakistan
M. Ahmad, M.I. Asghar, J. Butt, H.R. Hoorani, S. Khalid, W.A. Khan, T. Khurshid, S. Qazi, M.A. Shah, M. Shoaib

National Centre for Nuclear Research, Swierk, Poland
H. Bialkowska, B. Boimska, T. Frueboes, M. Górski, M. Kazana, K. Nawrocki, K. Romanowska-Rybinska, M. Szleper, G. Wrochna, P. Zalewski

Institute of Experimental Physics, Faculty of Physics, University of Warsaw, Warsaw, Poland
G. Brona, K. Bunkowski, M. Cwiok, W. Dominik, K. Doroba, A. Kalinowski, M. Konecki, J. Krolikowski, M. Misiura, W. Wolszczak

Laboratório de Instrumentação e Física Experimental de Partículas, Lisboa, Portugal
N. Almeida, P. Bargassa, C. Beirão Da Cruz E Silva, P. Faccioli, P.G. Ferreira Parracho, M. Gallinaro, F. Nguyen, J. Rodrigues Antunes, J. Seixas[2], J. Varela, P. Vischia

Joint Institute for Nuclear Research, Dubna, Russia
S. Afanasiev, P. Bunin, M. Gavrilenko, I. Golutvin, I. Gorbunov, A. Kamenev, V. Karjavin, V. Konoplyanikov, A. Lanev, A. Malakhov, V. Matveev, P. Moisenz, V. Palichik, V. Perelygin, S. Shmatov, N. Skatchkov, V. Smirnov, A. Zarubin

Petersburg Nuclear Physics Institute, Gatchina (St. Petersburg), Russia
S. Evstyukhin, V. Golovtsov, Y. Ivanov, V. Kim, P. Levchenko, V. Murzin, V. Oreshkin, I. Smirnov, V. Sulimov, L. Uvarov, S. Vavilov, A. Vorobyev, An. Vorobyev

Institute for Nuclear Research, Moscow, Russia
Yu. Andreev, A. Dermenev, S. Gninenko, N. Golubev, M. Kirsanov, N. Krasnikov, A. Pashenkov, D. Tlisov, A. Toropin

Institute for Theoretical and Experimental Physics, Moscow, Russia
V. Epshteyn, M. Erofeeva, V. Gavrilov, N. Lychkovskaya, V. Popov, G. Safronov, S. Semenov, A. Spiridonov, V. Stolin, E. Vlasov, A. Zhokin

P.N. Lebedev Physical Institute, Moscow, Russia
V. Andreev, M. Azarkin, I. Dremin, M. Kirakosyan, A. Leonidov, G. Mesyats, S.V. Rusakov, A. Vinogradov

Skobeltsyn Institute of Nuclear Physics, Lomonosov Moscow State University, Moscow, Russia
A. Belyaev, E. Boos, L. Dudko, A. Gribushin, L. Khein, V. Klyukhin, O. Kodolova, I. Lokhtin, A. Markina, S. Obraztsov, S. Petrushanko, A. Proskuryakov, V. Savrin, A. Snigirev

State Research Center of Russian Federation, Institute for High Energy Physics, Protvino, Russia
I. Azhgirey, I. Bayshev, S. Bitioukov, V. Kachanov, A. Kalinin, D. Konstantinov, V. Krychkine, V. Petrov, R. Ryutin, A. Sobol, L. Tourtchanovitch, S. Troshin, N. Tyurin, A. Uzunian, A. Volkov

University of Belgrade, Faculty of Physics and Vinca Institute of Nuclear Sciences, Belgrade, Serbia
P. Adzic[33], M. Djordjevic, M. Ekmedzic, D. Krpic[33], J. Milosevic

Centro de Investigaciones Energéticas Medioambientales y Tecnológicas (CIEMAT), Madrid, Spain
M. Aguilar-Benitez, J. Alcaraz Maestre, C. Battilana, E. Calvo, M. Cerrada, M. Chamizo Llatas[2], N. Colino, B. De La Cruz, A. Delgado Peris, D. Domínguez Vázquez, C. Fernandez Bedoya, J.P. Fernández Ramos, A. Ferrando, J. Flix, M.C. Fouz, P. Garcia-Abia, O. Gonzalez Lopez, S. Goy Lopez, J.M. Hernandez, M.I. Josa, G. Merino, E. Navarro De Martino, J. Puerta Pelayo, A. Quintario Olmeda, I. Redondo, L. Romero, J. Santaolalla, M.S. Soares, C. Willmott

Universidad Autónoma de Madrid, Madrid, Spain
C. Albajar, J.F. de Trocóniz

Universidad de Oviedo, Oviedo, Spain
H. Brun, J. Cuevas, J. Fernandez Menendez, S. Folgueras, I. Gonzalez Caballero, L. Lloret Iglesias, J. Piedra Gomez

Instituto de Física de Cantabria (IFCA), CSIC-Universidad de Cantabria, Santander, Spain
J.A. Brochero Cifuentes, I.J. Cabrillo, A. Calderon, S.H. Chuang, J. Duarte Campderros, M. Fernandez, G. Gomez, J. Gonzalez Sanchez, A. Graziano, C. Jorda, A. Lopez Virto, J. Marco, R. Marco, C. Martinez Rivero, F. Matorras, F.J. Munoz Sanchez, T. Rodrigo, A.Y. Rodríguez-Marrero, A. Ruiz-Jimeno, L. Scodellaro, I. Vila, R. Vilar Cortabitarte

CERN, European Organization for Nuclear Research, Geneva, Switzerland
D. Abbaneo, E. Auffray, G. Auzinger, M. Bachtis, P. Baillon, A.H. Ball, D. Barney, J. Bendavid, J.F. Benitez, C. Bernet[8], G. Bianchi, P. Bloch, A. Bocci, A. Bonato, O. Bondu, C. Botta, H. Breuker, T. Camporesi, G. Cerminara, T. Christiansen, J.A. Coarasa Perez, S. Colafranceschi[34], M. D'Alfonso, D. d'Enterria, A. Dabrowski, A. David, F. De Guio, A. De Roeck, S. De Visscher, S. Di Guida, M. Dobson, N. Dupont-Sagorin, A. Elliott-Peisert, J. Eugster, G. Franzoni, W. Funk, G. Georgiou, M. Giffels, D. Gigi, K. Gill, D. Giordano, M. Girone, M. Giunta, F. Glege, R. Gomez-Reino Garrido, S. Gowdy, R. Guida, J. Hammer, M. Hansen, P. Harris, C. Hartl, A. Hinzmann, V. Innocente, P. Janot, E. Karavakis, K. Kousouris, K. Krajczar, P. Lecoq, Y.-J. Lee, C. Lourenço, N. Magini, L. Malgeri, M. Mannelli, L. Masetti, F. Meijers, S. Mersi, E. Meschi, R. Moser, M. Mulders, P. Musella, E. Nesvold, L. Orsini, E. Palencia Cortezon, E. Perez, L. Perrozzi, A. Petrilli, A. Pfeiffer, M. Pierini, M. Pimiä, D. Piparo, M. Plagge, L. Quertenmont, A. Racz, W. Reece, G. Rolandi[35], M. Rovere, H. Sakulin, F. Santanastasio, C. Schäfer, C. Schwick,

S. Sekmen, A. Sharma, P. Siegrist, P. Silva, M. Simon, P. Sphicas[36], D. Spiga, M. Stoye, A. Tsirou, G.I. Veres[21], J.R. Vlimant, H.K. Wöhri, S.D. Worm[37], W.D. Zeuner

Paul Scherrer Institut, Villigen, Switzerland
W. Bertl, K. Deiters, W. Erdmann, K. Gabathuler, R. Horisberger, Q. Ingram, H.C. Kaestli, S. König, D. Kotlinski, U. Langenegger, D. Renker, T. Rohe

Institute for Particle Physics, ETH Zurich, Zurich, Switzerland
F. Bachmair, L. Bäni, L. Bianchini, P. Bortignon, M.A. Buchmann, B. Casal, N. Chanon, A. Deisher, G. Dissertori, M. Dittmar, M. Donegà, M. Dünser, P. Eller, K. Freudenreich, C. Grab, D. Hits, P. Lecomte, W. Lustermann, B. Mangano, A.C. Marini, P. Martinez Ruiz del Arbol, D. Meister, N. Mohr, F. Moortgat, C. Nägeli[38], P. Nef, F. Nessi-Tedaldi, F. Pandolfi, L. Pape, F. Pauss, M. Peruzzi, M. Quittnat, F.J. Ronga, M. Rossini, L. Sala, A.K. Sanchez, A. Starodumov[39], B. Stieger, M. Takahashi, L. Tauscher[†], A. Thea, K. Theofilatos, D. Treille, C. Urscheler, R. Wallny, H.A. Weber

Universität Zürich, Zurich, Switzerland
C. Amsler[40], V. Chiochia, C. Favaro, M. Ivova Rikova, B. Kilminster, B. Millan Mejias, P. Robmann, H. Snoek, S. Taroni, M. Verzetti, Y. Yang

National Central University, Chung-Li, Taiwan
M. Cardaci, K.H. Chen, C. Ferro, C.M. Kuo, S.W. Li, W. Lin, Y.J. Lu, R. Volpe, S.S. Yu

National Taiwan University (NTU), Taipei, Taiwan
P. Bartalini, P. Chang, Y.H. Chang, Y.W. Chang, Y. Chao, K.F. Chen, C. Dietz, U. Grundler, W.-S. Hou, Y. Hsiung, K.Y. Kao, Y.J. Lei, R.-S. Lu, D. Majumder, E. Petrakou, X. Shi, J.G. Shiu, Y.M. Tzeng, M. Wang

Chulalongkorn University, Bangkok, Thailand
B. Asavapibhop, N. Suwonjandee

Cukurova University, Adana, Turkey
A. Adiguzel, M.N. Bakirci[41], S. Cerci[42], C. Dozen, I. Dumanoglu, E. Eskut, S. Girgis, G. Gokbulut, E. Gurpinar, I. Hos, E.E. Kangal, A. Kayis Topaksu, G. Onengut[43], K. Ozdemir, S. Ozturk[41], A. Polatoz, K. Sogut[44], D. Sunar Cerci[42], B. Tali[42], H. Topakli[41], M. Vergili

Middle East Technical University, Physics Department, Ankara, Turkey
I.V. Akin, T. Aliev, B. Bilin, S. Bilmis, M. Deniz, H. Gamsizkan, A.M. Guler, G. Karapinar[45], K. Ocalan, A. Ozpineci, M. Serin, R. Sever, U.E. Surat, M. Yalvac, M. Zeyrek

Bogazici University, Istanbul, Turkey
E. Gülmez, B. Isildak[46], M. Kaya[47], O. Kaya[47], S. Ozkorucuklu[48], N. Sonmez[49]

Istanbul Technical University, Istanbul, Turkey
H. Bahtiyar[50], E. Barlas, K. Cankocak, Y.O. Günaydin[51], F.I. Vardarlı, M. Yücel

National Scientific Center, Kharkov Institute of Physics and Technology, Kharkov, Ukraine
L. Levchuk, P. Sorokin

University of Bristol, Bristol, United Kingdom
J.J. Brooke, E. Clement, D. Cussans, H. Flacher, R. Frazier, J. Goldstein, M. Grimes, G.P. Heath, H.F. Heath, L. Kreczko, C. Lucas, Z. Meng, S. Metson, D.M. Newbold[37], K. Nirunpong, S. Paramesvaran, A. Poll, S. Senkin, V.J. Smith, T. Williams

Rutherford Appleton Laboratory, Didcot, United Kingdom
K.W. Bell, A. Belyaev[52], C. Brew, R.M. Brown, D.J.A. Cockerill, J.A. Coughlan, K. Harder,

S. Harper, J. Ilic, E. Olaiya, D. Petyt, B.C. Radburn-Smith, C.H. Shepherd-Themistocleous, I.R. Tomalin, W.J. Womersley

Imperial College, London, United Kingdom
R. Bainbridge, O. Buchmuller, D. Burton, D. Colling, N. Cripps, M. Cutajar, P. Dauncey, G. Davies, M. Della Negra, W. Ferguson, J. Fulcher, D. Futyan, A. Gilbert, A. Guneratne Bryer, G. Hall, Z. Hatherell, J. Hays, G. Iles, M. Jarvis, G. Karapostoli, M. Kenzie, R. Lane, R. Lucas[37], L. Lyons, A.-M. Magnan, J. Marrouche, B. Mathias, R. Nandi, J. Nash, A. Nikitenko[39], J. Pela, M. Pesaresi, K. Petridis, M. Pioppi[53], D.M. Raymond, S. Rogerson, A. Rose, C. Seez, P. Sharp†, A. Sparrow, A. Tapper, M. Vazquez Acosta, T. Virdee, S. Wakefield, N. Wardle

Brunel University, Uxbridge, United Kingdom
M. Chadwick, J.E. Cole, P.R. Hobson, A. Khan, P. Kyberd, D. Leggat, D. Leslie, W. Martin, I.D. Reid, P. Symonds, L. Teodorescu, M. Turner

Baylor University, Waco, USA
J. Dittmann, K. Hatakeyama, A. Kasmi, H. Liu, T. Scarborough

The University of Alabama, Tuscaloosa, USA
O. Charaf, S.I. Cooper, C. Henderson, P. Rumerio

Boston University, Boston, USA
A. Avetisyan, T. Bose, C. Fantasia, A. Heister, P. Lawson, D. Lazic, J. Rohlf, D. Sperka, J. St. John, L. Sulak

Brown University, Providence, USA
J. Alimena, S. Bhattacharya, G. Christopher, D. Cutts, Z. Demiragli, A. Ferapontov, A. Garabedian, U. Heintz, S. Jabeen, G. Kukartsev, E. Laird, G. Landsberg, M. Luk, M. Narain, M. Segala, T. Sinthuprasith, T. Speer

University of California, Davis, Davis, USA
R. Breedon, G. Breto, M. Calderon De La Barca Sanchez, S. Chauhan, M. Chertok, J. Conway, R. Conway, P.T. Cox, R. Erbacher, M. Gardner, R. Houtz, W. Ko, A. Kopecky, R. Lander, T. Miceli, D. Pellett, J. Pilot, F. Ricci-Tam, B. Rutherford, M. Searle, J. Smith, M. Squires, M. Tripathi, S. Wilbur, R. Yohay

University of California, Los Angeles, USA
V. Andreev, D. Cline, R. Cousins, S. Erhan, P. Everaerts, C. Farrell, M. Felcini, J. Hauser, M. Ignatenko, C. Jarvis, G. Rakness, P. Schlein†, E. Takasugi, P. Traczyk, V. Valuev, M. Weber

University of California, Riverside, Riverside, USA
J. Babb, R. Clare, J. Ellison, J.W. Gary, G. Hanson, J. Heilman, P. Jandir, H. Liu, O.R. Long, A. Luthra, M. Malberti, H. Nguyen, A. Shrinivas, J. Sturdy, S. Sumowidagdo, R. Wilken, S. Wimpenny

University of California, San Diego, La Jolla, USA
W. Andrews, J.G. Branson, G.B. Cerati, S. Cittolin, D. Evans, A. Holzner, R. Kelley, M. Lebourgeois, J. Letts, I. Macneill, S. Padhi, C. Palmer, G. Petrucciani, M. Pieri, M. Sani, V. Sharma, S. Simon, E. Sudano, M. Tadel, Y. Tu, A. Vartak, S. Wasserbaech[54], F. Würthwein, A. Yagil, J. Yoo

University of California, Santa Barbara, Santa Barbara, USA
D. Barge, C. Campagnari, T. Danielson, K. Flowers, P. Geffert, C. George, F. Golf, J. Incandela, C. Justus, D. Kovalskyi, V. Krutelyov, R. Magaña Villalba, N. Mccoll, V. Pavlunin, J. Richman, R. Rossin, D. Stuart, W. To, C. West

California Institute of Technology, Pasadena, USA
A. Apresyan, A. Bornheim, J. Bunn, Y. Chen, E. Di Marco, J. Duarte, D. Kcira, Y. Ma, A. Mott, H.B. Newman, C. Pena, C. Rogan, M. Spiropulu, V. Timciuc, J. Veverka, R. Wilkinson, S. Xie, R.Y. Zhu

Carnegie Mellon University, Pittsburgh, USA
V. Azzolini, A. Calamba, R. Carroll, T. Ferguson, Y. Iiyama, D.W. Jang, Y.F. Liu, M. Paulini, J. Russ, H. Vogel, I. Vorobiev

University of Colorado at Boulder, Boulder, USA
J.P. Cumalat, B.R. Drell, W.T. Ford, A. Gaz, E. Luiggi Lopez, U. Nauenberg, J.G. Smith, K. Stenson, K.A. Ulmer, S.R. Wagner

Cornell University, Ithaca, USA
J. Alexander, A. Chatterjee, N. Eggert, L.K. Gibbons, W. Hopkins, A. Khukhunaishvili, B. Kreis, N. Mirman, G. Nicolas Kaufman, J.R. Patterson, A. Ryd, E. Salvati, W. Sun, W.D. Teo, J. Thom, J. Thompson, J. Tucker, Y. Weng, L. Winstrom, P. Wittich

Fairfield University, Fairfield, USA
D. Winn

Fermi National Accelerator Laboratory, Batavia, USA
S. Abdullin, M. Albrow, J. Anderson, G. Apollinari, L.A.T. Bauerdick, A. Beretvas, J. Berryhill, P.C. Bhat, K. Burkett, J.N. Butler, V. Chetluru, H.W.K. Cheung, F. Chlebana, S. Cihangir, V.D. Elvira, I. Fisk, J. Freeman, Y. Gao, E. Gottschalk, L. Gray, D. Green, O. Gutsche, D. Hare, R.M. Harris, J. Hirschauer, B. Hooberman, S. Jindariani, M. Johnson, U. Joshi, K. Kaadze, B. Klima, S. Kunori, S. Kwan, J. Linacre, D. Lincoln, R. Lipton, J. Lykken, K. Maeshima, J.M. Marraffino, V.I. Martinez Outschoorn, S. Maruyama, D. Mason, P. McBride, K. Mishra, S. Mrenna, Y. Musienko[55], C. Newman-Holmes, V. O'Dell, O. Prokofyev, N. Ratnikova, E. Sexton-Kennedy, S. Sharma, W.J. Spalding, L. Spiegel, L. Taylor, S. Tkaczyk, N.V. Tran, L. Uplegger, E.W. Vaandering, R. Vidal, J. Whitmore, W. Wu, F. Yang, J.C. Yun

University of Florida, Gainesville, USA
D. Acosta, P. Avery, D. Bourilkov, M. Chen, T. Cheng, S. Das, M. De Gruttola, G.P. Di Giovanni, D. Dobur, A. Drozdetskiy, R.D. Field, M. Fisher, Y. Fu, I.K. Furic, J. Hugon, B. Kim, J. Konigsberg, A. Korytov, A. Kropivnitskaya, T. Kypreos, J.F. Low, K. Matchev, P. Milenovic[56], G. Mitselmakher, L. Muniz, R. Remington, A. Rinkevicius, N. Skhirtladze, M. Snowball, J. Yelton, M. Zakaria

Florida International University, Miami, USA
V. Gaultney, S. Hewamanage, S. Linn, P. Markowitz, G. Martinez, J.L. Rodriguez

Florida State University, Tallahassee, USA
T. Adams, A. Askew, J. Bochenek, J. Chen, B. Diamond, J. Haas, S. Hagopian, V. Hagopian, K.F. Johnson, H. Prosper, V. Veeraraghavan, M. Weinberg

Florida Institute of Technology, Melbourne, USA
M.M. Baarmand, B. Dorney, M. Hohlmann, H. Kalakhety, F. Yumiceva

University of Illinois at Chicago (UIC), Chicago, USA
M.R. Adams, L. Apanasevich, V.E. Bazterra, R.R. Betts, I. Bucinskaite, J. Callner, R. Cavanaugh, O. Evdokimov, L. Gauthier, C.E. Gerber, D.J. Hofman, S. Khalatyan, P. Kurt, F. Lacroix, D.H. Moon, C. O'Brien, C. Silkworth, D. Strom, P. Turner, N. Varelas

The University of Iowa, Iowa City, USA
U. Akgun, E.A. Albayrak[50], B. Bilki[57], W. Clarida, K. Dilsiz, F. Duru, S. Griffiths, J.-P. Merlo, H. Mermerkaya[58], A. Mestvirishvili, A. Moeller, J. Nachtman, C.R. Newsom, H. Ogul, Y. Onel, F. Ozok[50], S. Sen, P. Tan, E. Tiras, J. Wetzel, T. Yetkin[59], K. Yi

Johns Hopkins University, Baltimore, USA
B.A. Barnett, B. Blumenfeld, S. Bolognesi, G. Giurgiu, A.V. Gritsan, G. Hu, P. Maksimovic, C. Martin, M. Swartz, A. Whitbeck

The University of Kansas, Lawrence, USA
P. Baringer, A. Bean, G. Benelli, R.P. Kenny III, M. Murray, D. Noonan, S. Sanders, R. Stringer, J.S. Wood

Kansas State University, Manhattan, USA
A.F. Barfuss, I. Chakaberia, A. Ivanov, S. Khalil, M. Makouski, Y. Maravin, L.K. Saini, S. Shrestha, I. Svintradze

Lawrence Livermore National Laboratory, Livermore, USA
J. Gronberg, D. Lange, F. Rebassoo, D. Wright

University of Maryland, College Park, USA
A. Baden, B. Calvert, S.C. Eno, J.A. Gomez, N.J. Hadley, R.G. Kellogg, T. Kolberg, Y. Lu, M. Marionneau, A.C. Mignerey, K. Pedro, A. Peterman, A. Skuja, J. Temple, M.B. Tonjes, S.C. Tonwar

Massachusetts Institute of Technology, Cambridge, USA
A. Apyan, G. Bauer, W. Busza, I.A. Cali, M. Chan, L. Di Matteo, V. Dutta, G. Gomez Ceballos, M. Goncharov, D. Gulhan, Y. Kim, M. Klute, Y.S. Lai, A. Levin, P.D. Luckey, T. Ma, S. Nahn, C. Paus, D. Ralph, C. Roland, G. Roland, G.S.F. Stephans, F. Stöckli, K. Sumorok, D. Velicanu, R. Wolf, B. Wyslouch, M. Yang, Y. Yilmaz, A.S. Yoon, M. Zanetti, V. Zhukova

University of Minnesota, Minneapolis, USA
B. Dahmes, A. De Benedetti, A. Gude, J. Haupt, S.C. Kao, K. Klapoetke, Y. Kubota, J. Mans, N. Pastika, R. Rusack, M. Sasseville, A. Singovsky, N. Tambe, J. Turkewitz

University of Mississippi, Oxford, USA
J.G. Acosta, L.M. Cremaldi, R. Kroeger, S. Oliveros, L. Perera, R. Rahmat, D.A. Sanders, D. Summers

University of Nebraska-Lincoln, Lincoln, USA
E. Avdeeva, K. Bloom, S. Bose, D.R. Claes, A. Dominguez, M. Eads, R. Gonzalez Suarez, J. Keller, I. Kravchenko, J. Lazo-Flores, S. Malik, F. Meier, G.R. Snow

State University of New York at Buffalo, Buffalo, USA
J. Dolen, A. Godshalk, I. Iashvili, S. Jain, A. Kharchilava, A. Kumar, S. Rappoccio, Z. Wan

Northeastern University, Boston, USA
G. Alverson, E. Barberis, D. Baumgartel, M. Chasco, J. Haley, A. Massironi, D. Nash, T. Orimoto, D. Trocino, D. Wood, J. Zhang

Northwestern University, Evanston, USA
A. Anastassov, K.A. Hahn, A. Kubik, L. Lusito, N. Mucia, N. Odell, B. Pollack, A. Pozdnyakov, M. Schmitt, S. Stoynev, K. Sung, M. Velasco, S. Won

University of Notre Dame, Notre Dame, USA
D. Berry, A. Brinkerhoff, K.M. Chan, M. Hildreth, C. Jessop, D.J. Karmgard, J. Kolb, K. Lannon,

W. Luo, S. Lynch, N. Marinelli, D.M. Morse, T. Pearson, M. Planer, R. Ruchti, J. Slaunwhite, N. Valls, M. Wayne, M. Wolf

The Ohio State University, Columbus, USA
L. Antonelli, B. Bylsma, L.S. Durkin, C. Hill, R. Hughes, K. Kotov, T.Y. Ling, D. Puigh, M. Rodenburg, G. Smith, C. Vuosalo, B.L. Winer, H. Wolfe

Princeton University, Princeton, USA
E. Berry, P. Elmer, V. Halyo, P. Hebda, J. Hegeman, A. Hunt, P. Jindal, S.A. Koay, P. Lujan, D. Marlow, T. Medvedeva, M. Mooney, J. Olsen, P. Piroué, X. Quan, A. Raval, H. Saka, D. Stickland, C. Tully, J.S. Werner, S.C. Zenz, A. Zuranski

University of Puerto Rico, Mayaguez, USA
E. Brownson, A. Lopez, H. Mendez, J.E. Ramirez Vargas

Purdue University, West Lafayette, USA
E. Alagoz, D. Benedetti, G. Bolla, D. Bortoletto, M. De Mattia, A. Everett, Z. Hu, M. Jones, K. Jung, O. Koybasi, M. Kress, N. Leonardo, D. Lopes Pegna, V. Maroussov, P. Merkel, D.H. Miller, N. Neumeister, I. Shipsey, D. Silvers, A. Svyatkovskiy, F. Wang, W. Xie, L. Xu, H.D. Yoo, J. Zablocki, Y. Zheng

Purdue University Calumet, Hammond, USA
N. Parashar

Rice University, Houston, USA
A. Adair, B. Akgun, K.M. Ecklund, F.J.M. Geurts, W. Li, B. Michlin, B.P. Padley, R. Redjimi, J. Roberts, J. Zabel

University of Rochester, Rochester, USA
B. Betchart, A. Bodek, R. Covarelli, P. de Barbaro, R. Demina, Y. Eshaq, T. Ferbel, A. Garcia-Bellido, P. Goldenzweig, J. Han, A. Harel, D.C. Miner, G. Petrillo, D. Vishnevskiy, M. Zielinski

The Rockefeller University, New York, USA
A. Bhatti, R. Ciesielski, L. Demortier, K. Goulianos, G. Lungu, S. Malik, C. Mesropian

Rutgers, The State University of New Jersey, Piscataway, USA
S. Arora, A. Barker, J.P. Chou, C. Contreras-Campana, E. Contreras-Campana, D. Duggan, D. Ferencek, Y. Gershtein, R. Gray, E. Halkiadakis, D. Hidas, A. Lath, S. Panwalkar, M. Park, R. Patel, V. Rekovic, J. Robles, S. Salur, S. Schnetzer, C. Seitz, S. Somalwar, R. Stone, S. Thomas, P. Thomassen, M. Walker

University of Tennessee, Knoxville, USA
G. Cerizza, M. Hollingsworth, K. Rose, S. Spanier, Z.C. Yang, A. York

Texas A&M University, College Station, USA
O. Bouhali[60], R. Eusebi, W. Flanagan, J. Gilmore, T. Kamon[61], V. Khotilovich, R. Montalvo, I. Osipenkov, Y. Pakhotin, A. Perloff, J. Roe, A. Safonov, T. Sakuma, I. Suarez, A. Tatarinov, D. Toback

Texas Tech University, Lubbock, USA
N. Akchurin, C. Cowden, J. Damgov, C. Dragoiu, P.R. Dudero, K. Kovitanggoon, S.W. Lee, T. Libeiro, I. Volobouev

Vanderbilt University, Nashville, USA
E. Appelt, A.G. Delannoy, S. Greene, A. Gurrola, W. Johns, C. Maguire, Y. Mao, A. Melo, M. Sharma, P. Sheldon, B. Snook, S. Tuo, J. Velkovska

University of Virginia, Charlottesville, USA
M.W. Arenton, S. Boutle, B. Cox, B. Francis, J. Goodell, R. Hirosky, A. Ledovskoy, C. Lin, C. Neu, J. Wood

Wayne State University, Detroit, USA
S. Gollapinni, R. Harr, P.E. Karchin, C. Kottachchi Kankanamge Don, P. Lamichhane, A. Sakharov

University of Wisconsin, Madison, USA
D.A. Belknap, L. Borrello, D. Carlsmith, M. Cepeda, S. Dasu, S. Duric, E. Friis, M. Grothe, R. Hall-Wilton, M. Herndon, A. Hervé, P. Klabbers, J. Klukas, A. Lanaro, R. Loveless, A. Mohapatra, I. Ojalvo, T. Perry, G.A. Pierro, G. Polese, I. Ross, T. Sarangi, A. Savin, W.H. Smith, J. Swanson

†: Deceased
1: Also at Vienna University of Technology, Vienna, Austria
2: Also at CERN, European Organization for Nuclear Research, Geneva, Switzerland
3: Also at Institut Pluridisciplinaire Hubert Curien, Université de Strasbourg, Université de Haute Alsace Mulhouse, CNRS/IN2P3, Strasbourg, France
4: Also at National Institute of Chemical Physics and Biophysics, Tallinn, Estonia
5: Also at Skobeltsyn Institute of Nuclear Physics, Lomonosov Moscow State University, Moscow, Russia
6: Also at Universidade Estadual de Campinas, Campinas, Brazil
7: Also at California Institute of Technology, Pasadena, USA
8: Also at Laboratoire Leprince-Ringuet, Ecole Polytechnique, IN2P3-CNRS, Palaiseau, France
9: Also at Zewail City of Science and Technology, Zewail, Egypt
10: Also at Suez Canal University, Suez, Egypt
11: Also at Cairo University, Cairo, Egypt
12: Also at Fayoum University, El-Fayoum, Egypt
13: Also at British University in Egypt, Cairo, Egypt
14: Now at Ain Shams University, Cairo, Egypt
15: Also at National Centre for Nuclear Research, Swierk, Poland
16: Also at Université de Haute Alsace, Mulhouse, France
17: Also at Joint Institute for Nuclear Research, Dubna, Russia
18: Also at Brandenburg University of Technology, Cottbus, Germany
19: Also at The University of Kansas, Lawrence, USA
20: Also at Institute of Nuclear Research ATOMKI, Debrecen, Hungary
21: Also at Eötvös Loránd University, Budapest, Hungary
22: Also at Tata Institute of Fundamental Research - EHEP, Mumbai, India
23: Also at Tata Institute of Fundamental Research - HECR, Mumbai, India
24: Now at King Abdulaziz University, Jeddah, Saudi Arabia
25: Also at University of Visva-Bharati, Santiniketan, India
26: Also at University of Ruhuna, Matara, Sri Lanka
27: Also at Isfahan University of Technology, Isfahan, Iran
28: Also at Sharif University of Technology, Tehran, Iran
29: Also at Plasma Physics Research Center, Science and Research Branch, Islamic Azad University, Tehran, Iran
30: Also at Università degli Studi di Siena, Siena, Italy
31: Also at Purdue University, West Lafayette, USA
32: Also at Universidad Michoacana de San Nicolas de Hidalgo, Morelia, Mexico
33: Also at Faculty of Physics, University of Belgrade, Belgrade, Serbia

34: Also at Facoltà Ingegneria, Università di Roma, Roma, Italy
35: Also at Scuola Normale e Sezione dell'INFN, Pisa, Italy
36: Also at University of Athens, Athens, Greece
37: Also at Rutherford Appleton Laboratory, Didcot, United Kingdom
38: Also at Paul Scherrer Institut, Villigen, Switzerland
39: Also at Institute for Theoretical and Experimental Physics, Moscow, Russia
40: Also at Albert Einstein Center for Fundamental Physics, Bern, Switzerland
41: Also at Gaziosmanpasa University, Tokat, Turkey
42: Also at Adiyaman University, Adiyaman, Turkey
43: Also at Cag University, Mersin, Turkey
44: Also at Mersin University, Mersin, Turkey
45: Also at Izmir Institute of Technology, Izmir, Turkey
46: Also at Ozyegin University, Istanbul, Turkey
47: Also at Kafkas University, Kars, Turkey
48: Also at Suleyman Demirel University, Isparta, Turkey
49: Also at Ege University, Izmir, Turkey
50: Also at Mimar Sinan University, Istanbul, Istanbul, Turkey
51: Also at Kahramanmaras Sütcü Imam University, Kahramanmaras, Turkey
52: Also at School of Physics and Astronomy, University of Southampton, Southampton, United Kingdom
53: Also at INFN Sezione di Perugia; Università di Perugia, Perugia, Italy
54: Also at Utah Valley University, Orem, USA
55: Also at Institute for Nuclear Research, Moscow, Russia
56: Also at University of Belgrade, Faculty of Physics and Vinca Institute of Nuclear Sciences, Belgrade, Serbia
57: Also at Argonne National Laboratory, Argonne, USA
58: Also at Erzincan University, Erzincan, Turkey
59: Also at Yildiz Technical University, Istanbul, Turkey
60: Also at Texas A&M University at Qatar, Doha, Qatar
61: Also at Kyungpook National University, Daegu, Korea